RSC Advances

REVIEW

View Article Online
View Journal | View Issue

Cite this: *RSC Adv.*, 2017, **7**, 1782

Post-synthetic ion-exchange process in nanoporous metal–organic frameworks; an effective way for modulating their structures and properties

Yasamin Noori and Kamran Akhbari*

Over the last two decades, metal–organic frameworks (MOFs) have received great attention and the number of compounds reported is still growing, which is mainly due to their amazing structures and various pore topologies, accessible cages and their potential applications in different fields, such as gas storage, separation, ion-exchange and catalysis. Among these, ion-exchange processes are considered as the post-synthetic parturient technique as it can achieve dominant applications. There are two primary types of ion-exchange processes (anionic and cationic) and each type may use naturally occurring and synthetic materials. The cation-exchange process at the SBUs of MOFs and metal-exchange involving metal nodes in MOFs, have been previously reported. In this study, we attempt to give an overview of all types of ion-exchange processes that occur in the pores and study their applications. We studied the aspects relating to the new MOFs that are driven during their use in ion-exchange: for example, why ion-exchange occurs, a comparison between the MOFs before and after the ion-exchange process and their current applications.

Received 9th October 2016
Accepted 1st December 2016

DOI: 10.1039/c6ra24958b

www.rsc.org/advances

1. Introduction

Over the last two decades, supramolecular compounds have monopolized the attention of researchers and the number of

School of Chemistry, College of Science, University of Tehran, P. O. Box 14155-6455, Tehran, Islamic Republic of Iran. E-mail: akhbari.k@khayam.ut.ac.ir; Fax: +98 21 66495291; Tel: +98 21 61113734

Yasamin Noori was born in Tehran, Iran. She received her Bachelor's Degree in Pure Chemistry from the University of Tehran. Yasamin is currently a second year student at the University of Tehran working towards earning her Master of Science Degree in Nano-chemistry. She works under the guidance of Assistant Professor Kamran Akhbari and her research focused on the post-synthetic ion-exchange process in nanoporous metal–organic frameworks and the solid-state structural transformations of lead(II) and cadmium(II) coordination polymers and supramolecular compounds using mechanochemical methods.

Kamran Akhbari joined the Department of Chemistry of the University of Tehran in 2013. He earned a Bachelor's Degree in Chemistry from Shahid Beheshti University in 2005, a Master of Science Degree in 2008 and PhD Degree in 2012 in Inorganic Chemistry from Tarbiat Modares University. He passed a post-doctoral fellow under the supervision of Prof. Ali Morsali at Tarbiat Modares University. He has published more than sixty papers and his current research focuses on the crystal engineering of coordination polymers and supramolecular compounds, metal–organic frameworks (MOFs) and their potential applications in energy storage materials, separation, drug delivery and catalysis. In 2013, he won the second place in the Khwarizmi Young Award for his work in the field of modulating methane storage in nanoporous anionic MOFs via a post-synthetic cation-exchange process.

their compounds being synthesized is still growing.[1–3] A wide branch of supramolecular compounds is "coordination polymers". CPs are obtained from the coordination bonds formed between metal centers and appropriate ligands.[4] CPs offer significant advantages over conventional molecular compounds due to their very low solubility in conventional organic solvents and water and much higher thermal stability.[1,5] Recently, CP nanocrystals, with finite repeating units, have aroused a growing interest due to their particular properties that differ from the conventional bulk CP.[6–9] As the prototype of polymeric crystal engineering, CPs are an intriguing class of hybrid materials, which exist as infinite crystalline lattices extended from inorganic vertices (metal ions or clusters) and organic ligand struts *via* coordination interactions.[10] The structure and properties of coordination polymers depend on the coordination habits and geometries of both metal ions and connecting ligands.[11,12] Metal coordination polymers represent an important interface between synthetic chemistry and materials science.[13] Metal–organic coordination polymer is a general term used to indicate an infinite array of metal ions linked by coordinated ligands.[13] A coordination compound is any compound that contains a coordination entity. A coordination entity is an ion or neutral molecule that is comprised of a central atom, usually that of a metal, to which is attached a surrounding array of atoms or groups of atoms, each of which is called a ligand.[14]

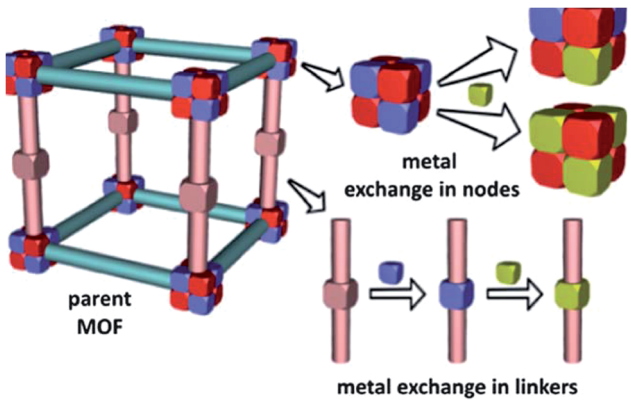

Fig. 1 Metal-exchange within MOF nodes and metal-exchange in metal-containing linkers. Reproduced with permission from ref. 39, copyright 2013, Royal Society of Chemistry.

This is a general term that incorporates a wide range of architectures including simple one-dimensional chains[15] with small ligands to large mesoporous frameworks like metal–organic frameworks.[16] The diversity in both the focus and scientific basis of the researchers involved has led to numerous terminology suggestions and practices for this class of compounds and several subgroups within them. While "coordination" seems entirely reasonable to use at this level, a generic term describing both 2D- and 3D-coordination polymers namely "coordination network solids" may be useful.[17] Porous metal–organic frameworks are zeolite analogues with constant porosity and adsorption capacity.[18] In the formation of MOFs, several parameters are involved, such as the metal and its coordination possibilities, the nature of the counter anion, the metal-to-ligand ratio and flexibility of the organic building blocks.[19] MOFs have attracted a substantial amount of attention because of their unique properties as highly tailorable microporous materials[20] and their applications in gas sorption,[21–23] catalysis,[24–27] separation,[28,29] drug delivery,[30,31] and the synthesis of nanomaterials.[32–34] Ion-exchange is one of the interesting properties of anionic or cationic MOFs that do not have neutral frameworks.[35–38] To date, two bunches of exchange that occur in the metal nodes and secondary building units (SBUs) of MOFs, have been studied. In the first group, metal-exchange involving metal nodes and metalated struts in MOFs has been reported. Their discussion focused on the system where metal cations are exchanged directly in the node (Fig. 1).[39]

The other group studied the cation-exchange occurring in the SBUs of MOF's. They also limited their discussion to the substitution that occurs at the SBUs and not in the pores.[40] In addition, both of them studied cation-exchange, while the ion-exchange that occurs at MOFs is not confined to cation-exchange. Recently, post-synthetic exchange (PSE) of MOFs through the metathesis of organic linkers has been discovered, as well as metal ions in the SBUs of MOFs (Fig. 2) have been revealed.[41,42] Similar cation and anion-exchange reactions with nanoparticles and other inorganic materials have been apperceived; however, the observation of a likewise phenomenon in MOFs is relatively novel.[43] There are two primary types of ion-exchange, organic and inorganic. Most inorganic ion-exchanges occur in small pore sizes and thus, the kinetics of the ion-exchange is slow, though organic exchangers, such as polymer resins, display rapid ion-exchange.[44]

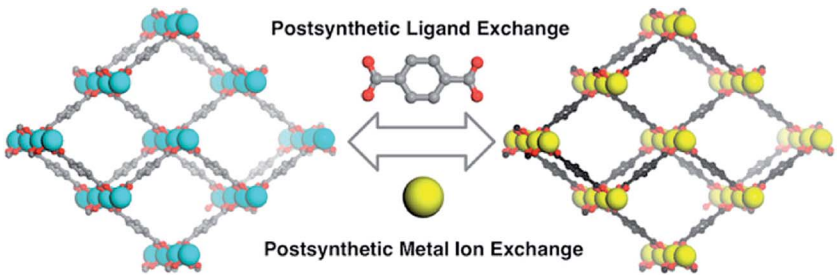

Fig. 2 Post-synthetic ligand and metal ion-exchange (PSE) processes. Reproduced with permission from ref. 42, copyright 2012, American Chemical Society.

In the other aspect, ion-exchange can be divided into cation-exchange and anion-exchange. This study outlines the available observations of all types of exchange that occurs in the pores of MOFs and the general trends and future studies can be outlined. We organized the data around cation-exchange and anion-exchange. All known examples of substitution in the MOFs pores and relevant details are reported. We also note that we have limited our discussion to the exchange that occurs in the pores and not at the SBUs or nodes. In addition, we focused on the applications that have been attained through ion-exchange, such as the separation of gases, catalysis, adsorption and luminescence properties. A comparison between MOFs has also been carried out in these cited cases *via* ion-exchange. Ion-exchange has already yielded some amazing results and new materials that have not been accessible otherwise, but the limit of its use for architecting new MOFs in a systematic and predictive manner depends on understanding its mechanism. This tutorial review is envisaged to provide a blueprint towards this goal.

2. Ion-exchange in metal–organic frameworks

To prepare metal–organic frameworks, a wide range of metal centers and multi-purpose organic ligands, which can be befitted for ion-exchange have been used.[45] If we can predict which MOFs are capable to ion-exchange, it will become a logical tool for synthesizing new materials with targeted properties. When the factors that generate exchangeable ions in the pores are elucidated, particular materials may be selected for ion-exchange including cation-exchange and anion-exchange, and their exact compounds may be designed. In this section, we classify two branches of ion-exchange based on their examples, reported cases and their applications.

2.1 Anion-exchange

In this content, it has been well known that the counter ions can play an important role in the coordination interactions[46] and for MOFs that have cationic coordination frameworks, the anions are generally included for charge balance and/or serve as templates in the empty spaces available. As a result, the anion-exchange properties for such MOF materials have been extensively investigated (Fig. 3).[47] In addition, if a neutral open framework can be oxidized, it will contain free counter anions in the channels or pores, which may be applied in anion-exchange materials.[35]

2.1.1 Early examples of anion-exchange. A neutral framework can be oxidized and then applied in anion-exchange materials. In this case, (BOF-1,1) (**1**) has been reported. (BOF-1,1) (**1**) was assembled from a bismacrocyclic nickel(II) complex and (Na_3BTC). The researchers carried out a redox reaction on **1** using I_2 to change the function of BOF_1 from guest recognition to ion-exchange reaction with I_2, two-thirds of the nickel(II) ions contained in the framework of **1** were oxidized to low spin nickel(III) and the I_2 molecules were reduced to I_3^- anions, which were included the pores of the framework (Fig. 4).

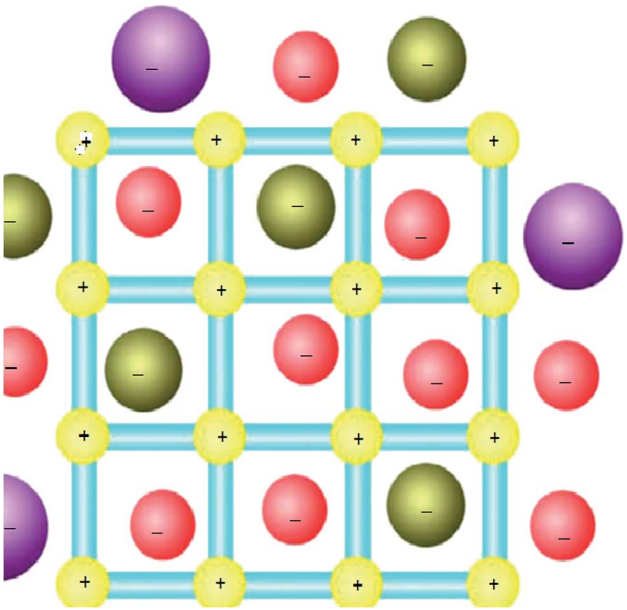

Fig. 3 The MOFs-based ion-exchange system (with a cationic framework). Reproduced with permission from ref. 47, copyright 2013, Nature publishing group.

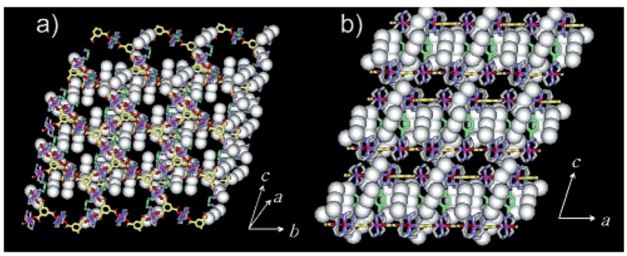

Fig. 4 The X-ray structure showing oxidized framework with I_3^- and I_2 included in the channels. (a) Top-view. (b) Side-view. Reproduced with permission from ref. 49, copyright 2004, American Chemical Society.

The redox reaction was performed to obtain a positively charged bilayer framework including free counter anions and the resulting product was applied to anion-exchange.[48] This compound is comprised of exchangeable free I_3^- anions located in the channels.[49]

As another example, a new MOF with zeolite topology, constructed from a tetrahedral building block, has been reported. The novel open-framework metal–organic polymer was $[\{Cd(H_2O)_3\}_{34}(N_4C_6H_{12})_{17}]Cl_{68}\cdot 46H_2O\cdot 68DMF$ (**2**). Anion-exchange was carried out for the cationic framework by substituting SCN^- for Cl^- in the cages.[50]

Several dipyrromethane (dipyrrinato, diprrin) coordination complexes that are generally used to prepare the structures found in a class of organic ligand MOFs reported before,[51] have been described by X. Z. Kiang *et al.* In addition, they have reported a more executive and systematic investigation of these dipyrin-based metalloligand systems describing 14 new MOF structures. The topology generated upon the formation of the MOFs was found to be robust in certain cases, as demonstrated

by anion-exchange. Among the 14 new MOFs, anion-exchange of (MOF-Co/$AgBF_4$-1) (**3**) and (MOF-Co/AgoTf-1) (**4**) has been investigated. Crystals of **4** were grown according to the procedures used to prepare **3**. Once single crystals were formed, the mother liquid was removed and replaced with a solution of tetrabutylammonium tetrafluoroborate quickly. An identical experiment was performed using MOF **4** and tetrabutylammonium hexafluorophospate. In this case, the PF_6^- anion was exchanged. The ability of the large PF_6^- anion to completely replace the triflate anion in **4** strongly suggests that the template effect observed in this MOF was not exclusively due to the size of the anion. In their experiment, during the anion-exchange process, no change in crystal morphology or stability was observed. The PF_6^- anions occupy the same positions in the crystal lattice as the displaced triflate anions (Fig. 5).[52]

A novel polymeric coordination complex $[Ni(timpt)_2](ClO_4)_2$ (**5**) has been synthesized *via* a solvothermal reaction using a template ligand with $Ni(ClO_4)_2 \cdot 6H_2O$ by Sh. Y. Wan and co-workers. The anion-exchange of this MOF is another studied case. Their research was the first example of a self-penetrating MOF that was established from a flexible three-connecting ligand. The powder of this MOF was suspended in an aqueous solution of $NaNO_3$ to allow possible anion-exchange process to occur. Both bands of NO_3^- and ClO_4^- anions have similar intensities. Among the anion-exchange, the ClO_4^- anions in the complex were exchanged with NO_3^- anions. The anion-exchange was also carried out using $NaBF_4$ and the same partial anion-exchange was observed.[53]

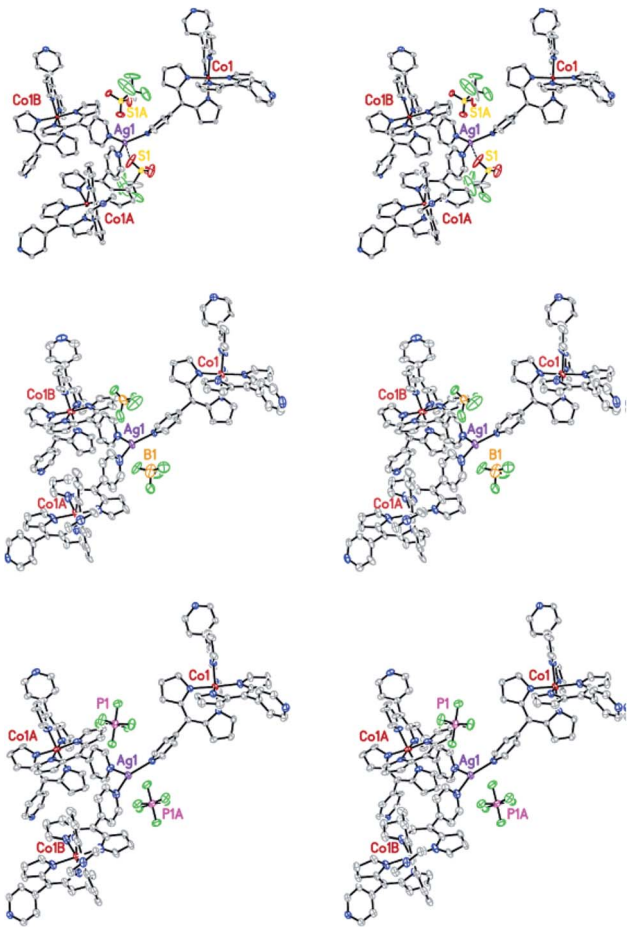

Fig. 5 The stereo-view of MOF-Co/AgOTf-1 highlighting the location of the anions before (top) and after anion-exchange. Reproduced with permission from ref. 52, copyright 2006, American Chemical Society.

Reversible anion-exchange of porous MOFs has also been studied. Two novel new rigid tripodal arene core based nitrogen ligands have been synthesized and used in the synthesis of $\{[Ag_3(1,3,5\text{-tris})_2X_2]X\}_n$ (X = ClO_4^- (**6**), X = NO_3^- (7)). The counter-ions located in the cationic frameworks can be exchanged reversibly. This observation indicates that these MOFs can act as zeolite-like porous materials for anion-exchange. The powder of the first MOF was suspended in water containing excess $NaNO_3$. The uncoordinated ClO_4^- ions exchange with the nitrate ions. To indicate the reversibility of the anion-exchange process in more detail, the exchanged solid was suspended in an aqueous solution of $NaClO_4$. It is very important to confirm that the anion exchange occurred in the solid state. Their experiments display the anion-exchange of this MOF occurs completely through the entire porous structure and was not just a surface phenomenon. The reversible anion-exchange for the second MOF was also carried out in the same way.[54]

Another study on selective anion-exchange properties has been recognized for a series of 3D microporous Cu coordination polymers. Their research describes a novel 3D MOF $\{[Cu(2\text{-}(2\text{-pyridyl}))_2](ClO_4)(H_2O)_{1/2}\}_n$ (**8**) and an unusual anion-exchange was observed for this material. In this case, the crystalline sample of MOF was suspended in an aqueous solution of NaX, where X represents the anion to be used in the exchange process. Notably, the ClO_4^- in the MOF can be completely replaced by $C_6H_5COO^-$. They also reported that the inverse anion-exchange reaction cannot be observed upon mixing the exchange product and $NaClO_4$ in water under similar conditions. Further experiments show that the ClO_4^- in the first MOF cannot be replaced by familiar inorganic anions, such as BF_4^-, OAc^-, NO_3^- and Cl^-, and even the other analogous organic carboxylates, such as O–CH_3–$C_6H_5COO^-$, *m*-CH_3–$C_6H_5COO^-$, *p*-$CH_3C_6H_5COO^-$, picolinate, nicotinate and isonicotinate.[55]

In other study, a research group proposed a rational approach to synthesize MOFs that include OH^- ions based on salt inclusion into alkaline-stable MOFs. Thus, they chose ZIF-8 (as the mother framework) and reported a novel MOF containing hydroxide ions $(NBU_4)_m(A)_n\{Zn(mim)_2\}_6$ (**9**). The NBU_4^+ ions are adequately stable in **9** for the MOF to impound the OH^- ions. To examine the anion-exchange of OH^- ions, the researchers stirred NSBU-ZIF-8 powder in an aqueous solution of NaOH and found that the included OH^- ions were exchangeable. Their experiment was the first example of a MOF including free OH^- ions. Other anions included in NBU_4-ZIF-8-OH were likely to be HCO_3^- or CO_3^{2-}. The existence of CO_3^{2-} ions probably inhibits the complete anion-exchange with OH^- ions.[56]

The last example involves the preparation of MOF [M(β-diketone)$_3$$Ag_3$]-$X_2$·solv (**10**). The most promising property of this network relies on its ability to exchange the anions present

in their channels. The research group selected $[ZnL_3Ag_3]X_2\cdot solv$ as the host network {X = BF_4^-, ClO_4^-, $CF_3SO_3^-$ and PF_6^-} and performed ion-exchange experiments using this material (Table 1). These anions can be easily exchanged in single-crystal to single-crystal processes.

Some preferences could also be elicited; for example (a) nitrate and perchlorate very readily displace BF_4^-, PF_6^- and triflate anions, (b) triflate is very ambulant and can be replaced by other anions and (c) triflate can be easily displaced using PF_6^-, while substitution of perchlorate was partial. The channel walls are covered by low-coordinated silver ions (UMCs) and these exposed centers can interact with anions. Other exchange experiments were carried out using organometallic complex anions. The anionic dinuclear organometallic complex $[Re_2(CO)_6(\mu\text{-}OH_3)]^-$ can be presented into 1D channels by exchange. In this case, the exchange was slower and after 1 day it was still only partial. This result of the group's experiments has opened the way to use their framework as a heterogeneous support for the foundation of organometallic compounds employed in homogeneous catalysis.[57]

2.2 Cation-exchange

Sometimes the exchange of metal ions or organic cations within anionic MOFs can modulate the chemical properties of a MOF[58,59] and this can be achieved simply by merging the sample into a solution containing a certain metal salt or organic cation to generate an anionic MOF. Prevalent ion-exchange resins with cationic groups and exchangeable counter ions are still the standard ion-exchange materials.[60] Porous zeolite-like metal–organic framework (ZMOF) materials with Rho and Sod topologies have also been studied. In the original ZMOFs, the negatively charged frameworks are charge-compensated by extra-framework ions inside the cavity, which can undergo ion-exchange with alkali metals.

2.2.1 Early examples of cation-exchange. A series of coordination metal–carboxylate frameworks have been synthesized using a flexible H_4X. However, the charged frameworks show some unique structures and properties compared to their neutral counterparts.[61] Some of the charged frameworks display ion-exchange for specific ions.[62] In this study, the reaction between divalent transition metal ions and H_4X ligands were reported. This reaction gave $[M_3X_2]\cdot[HDMA]_2\cdot 8DMA$ (M = Co (**11**), Mn (**12**)), which have anionic metal–carboxylate frameworks with $HDMA^+$ cations filled in the channels. Their observation illustrates that $HDMA^+$ in the channels of compounds **11** and **12** indicate ion-exchange behavior when treated with saturated aqueous solutions of $NaNO_3$ and KNO_3. The ion-exchange occurs with a color change from colorless to pink (Fig. 6). This means that the $HDMA^+$ cations within the channels of **11** and **12** can be replaced by the Na^+ ions in solution.[63]

In another case, the first example of a microporous MOF was reported by J. Yu and co-workers. The reaction of H_3BTB and $InCl_3$ in *N*,*N*-dimethyl formamide/1,4-dioxane/H_2O afforded colorless crystals of $(HDMA)_3[In_3(BTB)_4]\cdot 12DMF\cdot 22H_2O$ (ZJU-28) (**13**). The ion-exchange process studied showed that the cationic $Me_2NH_2^+$ molecules were readily exchanged by metal cations, such as Cu^{2+}, Ni^{2+} and Eu^{3+}. They examined the potential of **13** to encapsulate different pyridinium hemicyanine chromophores to expand non-linear optical MOF materials (Fig. 7).[64]

Four new MOFs based on flexible V-type tetracaboxylate ligands have been synthesized by Sh. Xiong and co-workers. On

Table 1 The inorganic anion-exchange process studied in the MOF $[ML_3Ag_3]$-$X_2\cdot solv$ (**10**). {Y = almost complete, P = partial, N = no exchange}

	$NaBF_4$	$NaClO_4$	$NaNO_3$	KPF_6
$[Zn^{II}L_3Ag_3](BF_4)_2$		Y	Y	P
$[Zn^{II}L_3Ag_3](ClO_4)_2$	N		P	P
$[Zn^{II}L_3Ag_3](CF_3SO_3)_2$	Y(30 min)	Y(2 h)	Y(15 min)	Y(2 h)
$[Zn^{II}L_3Ag_3](PF_6)_2$	P(24 h)	Y(3 h)	Y(2 h)	

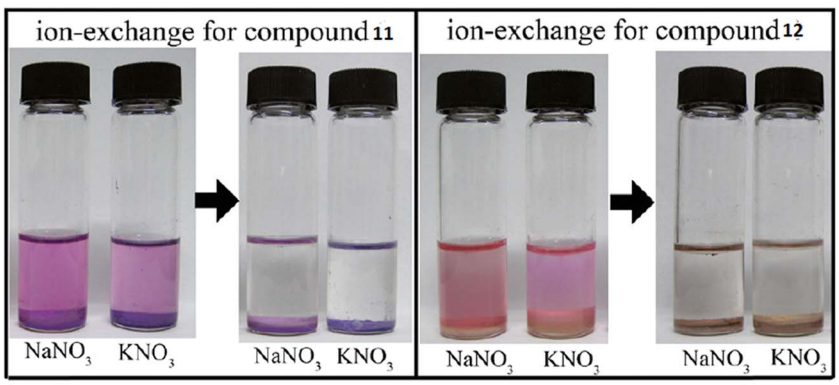

	Compound 11	Compound 12
Na^+	2.18%	3.17%
K^+	3.43%	3.58%

Fig. 6 Photographs of the ion-exchange process in compounds **11** and **12**. Reproduced with permission from ref. 63, copyright 2011, American Chemical Society.

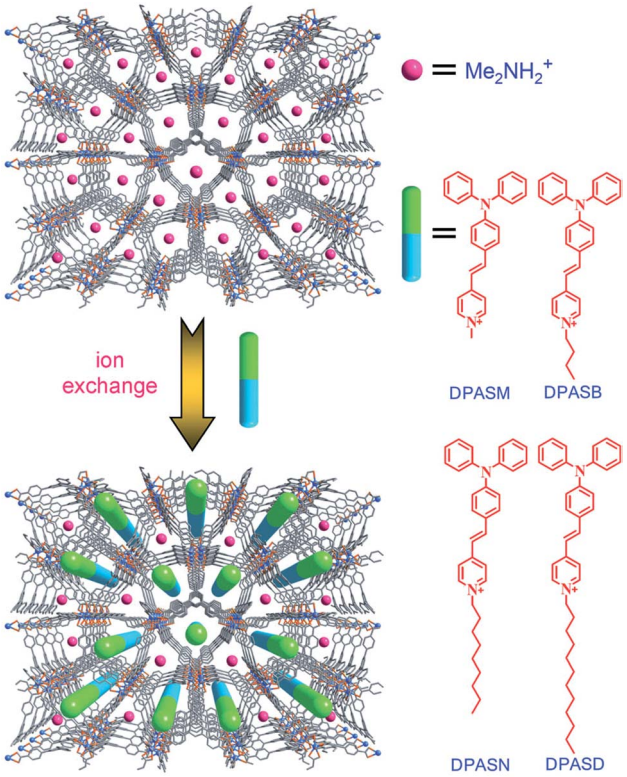

Fig. 7 A schematic of the pyridinium hemicyanine chromophores combined into ZJU-28. Reproduced with permission from ref. 64, copyright 2012, John Wiley & Sons.

the group of these MOFs, [HDMA] [In(mdip)]·2.5DMF·4H_2O (**14**) was a 3D anionic framework that exhibits selective metal ion-exchange of $HDMA^+$ ions with metal ions (M = Li^+, Na^+, K^+, Mg^{2+}, Ca^{2+}, Sr^{2+}, Ba^{2+}, Cu^{2+} and Fe^{3+}). Other work carried out by this group examined the selectivity of metal ion-exchange. The results indicated that Li^+ ions were hardly absorbed during the ion-exchange process. Perhaps this is the main reason of the high selectivity towards Na^+ and K^+ observed during the metal ion-exchange process. They proposed that the metal ions interact with the carboxylic oxygen atoms in compound **14**. The second group of metals used in the metal-ion exchange was Mg^{2+}, Ca^{2+}, Sr^{2+} and Ba^{2+}. Their observations indicate that compound **14** selectively adsorbs more Mg^{2+} than Ca^{2+}, Sr^{2+} and Ba^{2+}. As a result, the ion-exchange selectivity of the different metal ions was ascribed to the traits of the different metal ions and their interactions with the carboxylic oxygen atoms in the framework.[65]

Another research study on a series of isostructural metal–carboxylate frameworks [HDMA][M_2(bptc)(μ_3-OH)(H_2O)$_2$] (**15**) and cation-exchange of one of them with M = Co has been reported. This MOF has an anionic framework and 3D channels occupied by *in situ* generated $[HDMA]^+$ cations and was selected to perform ion-exchange experiments. The prepared crystals were immersed into a saturated solution of MCl (M = Li^+, Na^+, K^+). During this process, organic cations $[HDMA]^+$ can be selectively exchanged by alkali-metal cations. Interestingly, a comparison of the ion-exchange experiments showed that the crystal has a strange preference for Na^+ rather than for Li^+ and K^+. After ion-exchange with alkali cations, the crystals preserve their original shape although the surface roughness seems to increase. In addition, the intensity of the N–H bands of $[HDMA]^+$ during the exchange process was measured. After ion-exchange, the intensity of these bands became weak. All the experimental data show that alkali metal cations entered into the channels *via* an exchange interaction.[66]

Another MOF that has been studied is based on a high nuclearity cyclic-type cluster with a large internal cavity. The novel MOF is $H_2Na_4[Cu_{12}(OH)_6(PZ)_6(BTC)_6]\cdot 23H_2O$ (**16**) and the ion-exchange studies of this material have been reported. Because the framework in this MOF, contains large internal voids that contain in addition to solvent water molecules the Na^+ alkali metal cation, the cation-exchange properties of the crystal could be investigated through facile cation-exchange experiments. Ion exchange was performed with the alkali metal cations Li^+, K^+ and Cs^+ and transition metal cations Cu^{2+}, Ni^{2+} and Mn^{2+}.[67]

The synthesis of a gallium-based MOF [Ga_6(1,3,5-BTC)$_8$·6DMA·3DMF·26H_2O] (Ga·MOF-1) (**17**) is another example that has been regarded in this context. This MOF contains an anionic porous network. Disordered positively charged ions and solvent molecules are present in the pores. A porous anionic framework capable of ion-exchange is a potential precursor for adding alkali-metal cations into the pores.[68] These positively charged molecules can be exchanged with alkali-metal ions. Saturated solutions of $LiNO_3$ and $NaNO_3$ in DMF were separately added to the compound. Accordingly, the Li^+ and Na^+ ions were displaced. These results have confirmed that the presence of the cationic species within the pores make the MOF a suitable candidate for ion-exchange studies with alkali metal cations.[69]

Other compounds that have anionic frameworks are zeolite-like metal–organic frameworks (ZMOFs). Comparable to the prevalent inorganic zeolite, ZMOFs are anionic and show facile ionic exchange capacity. Ion-exchange studies show that the organic cations in the pores can be fully exchanged. Two important classes and topologies of ZMOF are Rho-ZMOF and Sod-ZMOF. The research group reported a novel strategy to construct ZMOFs with extra-large cavities. The extra-large cavities of {rho-ZMOF, HPP} [$In_{48}(C_5N_2O_4H_2)_{96}(C_2N_3H_{15})_{24}(DMF)_{36}(H_2O)_{192}$] (**18**) can adapt neutral molecules in addition to the cationic guest molecules that can only be exchanged with other cations. For Na^+-exchanged Rho-ZMOF formulated as [$Na_{48}{}^+(H_2O)_{282}$][$In_{48}(C_5N_2O_4H_2)_{96}$] (**19**), the concentration of charge carriers was higher than a typical rho zeolite. As a result, the anionic identity and the large approachable voids of Rho-ZMOF allowed the full exchange of the HPP cations with various organic and inorganic cations.[70]

Another research group has recently extended the design strategy that has allowed the construction of MOFs with zeolite-like topologies based on edge development. The synthesis of Rho-ZMOF, $In_{48}(C_5H_2N_2O_4)_{96}(C_7N_3H_{15})_{24}(C_3H_7NO)_{36}(H_2O)_{192}$ (**20**) and it's ion-exchange processes, in order to explore the potential application of this novel material, have also been investigated. They have displayed the ion-exchange of **20** in two

branches: (i) metal cation-exchange: the Na^+-exchange Rho-ZMOF was introduced; the ion-exchange data showed that the organic cations in the pores can be completely exchanged in an aqueous solution at room temperature. In addition, the Na^+-Rho-ZMOF indicated that the large amount of water molecules residing in the cages of the exchanged structure can be completely removed at temperatures around 100 °C. (ii) Organic cation-exchange: the large size of the cavities affiliated with Rho-ZMOF, together with the negative charge of the cavity internal, affords a chance to exchange and combine cationic organic molecules. In this case, they chose to exchange acridine orange (AO); the reason of this choice was its size. It is smaller than the window dimension of Rho-ZMOF and accordingly the molecules can freely diffuse into the large cavities.[71]

3. Applications of the ion-exchange process in metal–organic frameworks

3.1 Applications of the anion-exchange process

3.1.1 Separation process. The ion-exchange that has been introduced to date has some efficient applications. Some of these applications and the effects that occur after the exchange have been studied by different research groups. As an example, the synthesis of a series of positive indium MOFs and their use as a platform for an anion-exchange-based separation process have been reported. These MOFs are permanently porous MOFs with a positive framework (P-MOFs) with low stability or small pore size that only allows the exchange of small inorganic anions. A family of $[In_3O(COO)_6]^+$-based P-MOFs (ITCs) was prepared and used as the platform. The indium trimer-based cationic frameworks (ITCs) contain two different types of linear ditopic ligands: the mono-negative isonicotinate type ligand (L1, including (ina) and (pba)) and the di-negative terephthalate type ligand (L2, including (bdc), (NH_2-bdc), 2-bromoterephthalate, (ndc) and (bpdc)) in a 2 : 1 molar ratio. The anion exchange experiments were performed for the ITC-3 (**21**) and ITC-4 (**22**) MOFs using OG^{2-} as the anionic guest. The result showed that about 47.2% of the NO_3^- in **22** was replaced by OG^{2-} when the ion-exchange reached equilibrium after 4 days. The charge and size of the guest are the two most important factors in the ion-exchange process. Dyes were selected as the guest to study the ion-exchange process. In this study they arranged the organic dyes in two groups; the first group contained dyes with different charges but similar size (methylene blue, MLB^+; sudan I, SDI^0; acid orange 7, $AO7^-$; orange G, OG^{2-}; and new coccine, NC^{3-}), whereas, the dyes in the second group had different sizes, but same charges (OG^{2-}; ponceau 6R, $P6R^{2-}$; croscein scarlet 3B, $CS3B^{2-}$; croscein scarlet 7B, $CS7B^{2-}$; acid black 1, $AB1^{2-}$ and methyl blue, MB^{2-}). The separation process based on size- and charge-selective ion-exchange was mainly observed in the solutions containing two different dyes. Such selective anion-exchange, controlled by the structural characteristics of the MOFs, is advantageous and complementary to conventional ion-exchange resins because of its suitability for molecules within the ~100 Da < M_w < ~1000 Da range. Furthermore, the controlled release of guest anions make these P-MOFs potential candidates for use as drug carriers. The reticular synthesis and the large number of possible MOF structures make it possible to build an extensive library of hosts that can be used for guests (anionic in particular) of different sizes.[72]

In another study, a fluorene-based Cu(II)-MOF has been reported as a visual colorimetric anion sensor and separator based on anion-exchange $[CuL_2(H_2O)_{0.5}](NO_3)_2$ (**23**). The anion-exchange of this compound has also been studied. During the exchange, the NO_3^- anions can be replaced by other anions, such as: Cl^-, Br^-, I^-, SCN^- and N_3^-. The compound displayed a change in color as illustrated in Fig. 8a.

Compared to anion-exchange, the anion selectivity, catching a particular anion in the presence of other anionic competitors, is a more important task. As illustrated in Fig. 8b, the trigonal planar NO_3^- anion in compound **23** can be replaced by both spherical halide anions Cl^-, Br^- and I^-, and linear triatomic anions SCN^- and N_3^-, and therefore they envisioned that the compound can be used an anion separator to separate anions with similar geometry.[73]

The separation of anions from aqueous mixtures is another novel approach in this case. R. Custelcean, *et al.* presented a new approach for the separation of anions from water by their

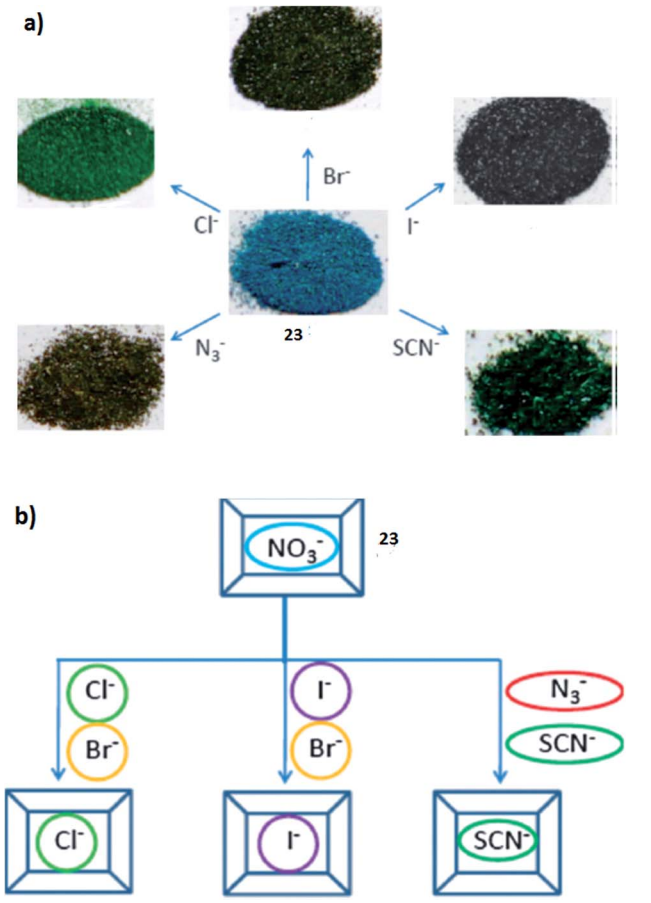

Fig. 8 (a) The color changes of compound $[CuL_2(H_2O)_{0.5}](NO_3)_2$ (**23**) as a result of anion-exchange. (b) The anion selectivity based on the compound. Reproduced with permission from ref. 73, copyright 2011, Royal Society of Chemistry.

selective crystallization within MOFs functionalized with urea hydrogen-bonding groups. One of the separation approaches that has been studied is the anion-exchange of $ZnCl_2$(BPu) (**24**), ZnI_2(BPu) (**25**) and $ZnBr_2$(BPu) (**26**). The most significant results of this study were that Cl^-, Br^- and I^- were exclusively crystallized against the ClO_4^-, NO_3^- and SO_4^{2-} oxo-anions, and the observed selectivity was opposite of the Hofmeister series typically governing the extraction of anions from water, whether by solvent extraction, anion-exchange with polymeric resins or coordination polymers.[74]

With the development of modern industry, anion pollutants have become a severe problem. Among the common anion pollutants, heavy-metal pollutants, normally in their oxo-/hydroxo anionic forms, such as $Cr_2O_7^{2-}$, MnO_4^-, pertechnetate (TcO_4^-), arsenate (AsO_4^{3-}) and selenite (SeO_3^{2-}, *etc.*) have been observed in water.[75] They have been a focus of concern because they cause serious damage to human health and the environment, which is a worldwide problem that is listed as a priority by the U.S. Environmental Protection Agency.[76] Recently, a few three-dimensional cationic MOFs have been used for the exchange and removal of heavy-metal pollutant anions, such as ReO_4^-, CrO_4^{2-} and TcO_4^-. One of these priority pollutants is chromate (CrO_4^{2-} or $Cr_2O_7^{2-}$): a known carcinogen, which originates from metal-plating, leather-tanning and other industries and is rapidly diffusing.[77] However, there have been few reports of $Cr_2O_7^{2-}$ anion exchange in MOFs despite the powerful carcinogenicity and extensive application of this species. Thus far, only several cationic MOFs have been reported to trap chromate or dichromate *via* ion-exchange. We studied all of these examples and have discussed them one by one. A 3d–4f heterometallic 3D cationic framework, $\{[Dy_2Zn(BPDC)_3(H_2O)_4](ClO_4)_2\cdot 10H_2O\}_n$ (**27**), which exhibits high thermal stability and strong alkali resistance has been reported. It is able to capture the pollutant CrO_4^{2-} unusually fast with a high capacity of 85%. According to the cationic framework and the large pores in **27**, several types of anions were selected to carry out the exchange experiments. 0.05 mmol of **27** was placed into a 0.05 mmol aqueous solution of K_2CrO_4 (10 mL) and the entire exchange process was performed under ambient conditions with slow stirring. Simultaneously, the color of the solid in the solution changed from colorless to yellow, implying the existence of CrO_4^{2-} in the solid. Similar exchange experiments were further carried out under an excess or very low concentration of K_2CrO_4. The results indicated that ClO_4^- in the channels was completely exchanged by CrO_4^{2-} under an excess concentration of K_2CrO_4. As is known, wastewater or nuclear waste contains more than one type of pollutant anion, such as halide ions or cyanide ions; therefore, it is indispensable to investigate whether **27** selectively exchanged CrO_4^{2-} from a mixture of anions. 0.05 mmol of **27** was immersed in a solution containing the mixed anions (NO_3^-, Cl^-, Br^-, I^- and CrO_4^{2-}) containing 0.1 mmol of each anion for 24 h. The results of the different analyses indicated that only ClO_4^- exchanged with CrO_4^{2-}, confirming its discrimination against halide ions. Generally, the release of pollutant anions is more difficult due to the strong interaction between the metal oxo-anions and cationic frameworks.[91] However, 57% and 25% CrO_4^{2-} in **27** can be released upon immersion in solutions of K_2CO_3 and Na_2SO_4, respectively, and no release in other NaX solutions (X = NO_3^-, Cl^-, Br^-, I^- and ClO_4^-) occurred.[78]

Another research group reported the unprecedented capacity and selectivity for trapping permanganate (MnO_4^-), perrhenate (ReO_4^-) and chromate (CrO_4^{2-}) using the cationic MOF, $Ag_2(4,4'\text{-bipy})_2(O_3SCH_2CH_2SO_3)\cdot 4H_2O$ (**28**). Unlike the strong affinity of LDHs for carbonate, **28** selectively trapped these problematic oxo-anion pollutants in record levels over all the previously reported materials. The mechanism of the high selectivity and adsorption capacity occurs *via* a crystal transition upon oxo-metal uptake. For a detailed investigation of the anion uptake capacity of **28**, permanganate and perrhenate were chosen as models for pertechnetate since all are group 7 oxo-anions. The as-synthesized **28** was introduced into a solution containing $KMnO_4$. In addition, the anion exchange reaction with commercially available synthetic hydrotalcite (magnesium aluminum hydroxycarbonate, Aldrich) in both the uncalcined and calcined form was carried out; after 48 h of exchange under the same conditions as in the case of **28**, only 3% and 18% of the anions were adsorbed by the LDHs, respectively.

The reason for the greater uptake by their material was due to crystal transformation by the host and the stability of the oxo-anion in the resultant structure, rather than a typical equilibrium-driven anion exchange. The as-synthesized **28** may also be used for anion exchange with a much higher adsorption capacity based on a stronger interaction towards the oxo-anion pollutant displayed by the resulting crystal structure, which can be seen to take the place at each end of the EDS molecule. The incoming permanganate anion plays a crucial role in high capacity trapping by forming a thermodynamically favorable crystal structure. Indeed, the same structure is formed if the nitrate- or perchlorate-containing version of **28** is used as the starting material. In order to further demonstrate the potential application of **28** towards pertechnetate abatement, perrhenate was also investigated. The resultant exchange solution was monitored only by ICP due to the overlap between EDS and perrhenate in the UV region. ReO_4^- trapping by **28** was even more rapid than that of MnO_4^-, reaching over 90% removal from solution in only 24 h, saturating in 48 h with 95% removal. Although the crystals were not suitable for single crystal analysis, the overall adsorption capacity of 1.90 (mol mol^{-1}) was comparable with the previous permanganate study, as expected. The adsorption capacity based on weight, however, reaches an exceptionally high value of 602 mg g^{-1} based on the molecular weight of ReO_4^- compared to that of MnO_4^-. Chromate exchange and adsorption capacity were also studied for **28**. UV-vis showed that 25%, 33%, and 41% of the chromate was exchanged after 8, 24, and 48 h, respectively. Moreover, the selectivity of anion trapping in **28** was studied with multiple competing anions of varying excess concentration in the presence of a low concentration of the target anion pollutant. A selective reaction with **28** was introduced into an aqueous solution comprised of $KMnO_4$ and $NaNO_3$. The measurements of the crystals after anion exchange indicated that only MnO_4^- entered the cationic material to replace the EDS anions. NO_3^- was not present inside the solid. The selectivity towards

perrhenate was also investigated with both of the competing nitrate and carbonate anions, with the same trapping behavior as permanganate. Perchlorate is another problematic anion that diffuses rapidly and widely and is emitted from rocket fuel waste along with other sources including pyrotechnics.[79] A mixed anion solution indicated that perchlorate was preferred over nitrate by **28**. The anion affinity for **28** thus displayed the following order, with the problematic metallate pollutants topping the list: MnO_4^- > ReO_4^- > ClO_4^- > CrO_4^{2-} > NO_3^- > CO_3^{2-}.[80]

The uptake capacities of dichromate ions in the MOFs have the potential to be improved, and the dichromate trapping processes of these MOFs are rarely known to occur in a single-crystal-to-single-crystal (SCSC) fashion. A research group reported two cationic MOFs with large nanotubular channels, $[Zn_2(Tipa)_2(OH)]\cdot 3NO_3\cdot 12H_2O$ (**29**) and $[Zn(Tipa)]\cdot 2NO_3\cdot DMF\cdot 4H_2O$ (**30**), which show fast ion-exchange and high uptake capacity for $Cr_2O_7^{2-}$ through an SCSC process. Given that **29** has a highly charged cationic layer structure, the anion exchange of oxo-anion pollutants was studied and chromate was chosen as an initial model. The anion exchange was performed under ambient conditions by simply placing crystals of **29** into the dichromate solution. The resultant exchange solution was monitored by liquid UV-vis spectroscopy and the result indicated that the $Cr_2O_7^{2-}$ in solution promptly entered into the channels of **29** by exchange with NO_3^-. Moreover, the color of the solid in the solution changed from colorless to yellow, implying the existence of $Cr_2O_7^{2-}$ in the solid. Similar ion-exchange experiments on **29** were further carried out in a solution of $K_2Cr_2O_7$, where 93.3% of dichromate in the solution was taken up by **29**. Subsequently, a slow decrease in the $Cr_2O_7^{2-}$ concentration was observed, and no further decrease in the anion concentration was detected after 10 h and 18 h. Release tests were also carried out to evaluate the regeneration ability of the ion-exchanger. For **29**, the samples were centrifuged, rinsed with water and dried in air after being submerged in a solution of dichromate. Then, the solid was placed in the same volume of solution in the presence of nitrate. Such a trapping and release process was performed for five continuous cycles and **29** still retained an approximately 87% release efficiency. Generally, it was understood that the release of the pollutant anions was more difficult due to the strong interactions between the metal oxo-anions and the cationic framework. The reversibility of **30** was also tested. Unlike **29**, there was almost no dichromate released in the presence of an excess of nitrate solution. In a solution of Na_2ClO_4, the exchange efficiency dropped to 63% after five trapping-release cycles. Selectivity is as important for anion trapping as is capacity. Given the high-capacity and rapid ion exchange function of **29**, the selective adsorption was verified. The dried sample of **29** was immersed in a solution containing mixed anions (Cl^-, Br^-, NO_3^-, and $Cr_2O_7^{2-}$). The results indicate that the adsorption of $Cr_2O_7^{2-}$ was not disturbed by the other ions. Nevertheless, when an equal molar amount of CO_3^{2-} was added to the abovementioned solution, the uptake efficiency of $Cr_2O_7^{2-}$ was reduced sharply to approximately 17%, indicating that the CO_3^{2-} ion was a strong competitor to the $Cr_2O_7^{2-}$ ion. When the dried sample of **29** was immersed into a solution containing mixed anions (Cl^-, Br^- and NO_3^- at concentrations of 0.10 mmol L^{-1} or 0.40 mmol L^{-1}, and $Cr_2O_7^{2-}$ at a concentration of 0.01 mmol L^{-1}), the adsorption of $Cr_2O_7^{2-}$ was still at a high efficiency. Once more, the dried sample of **29** was immersed in the mixed solution (Cl^-, Br^-, NO_3^-, SO_4^{2-} and ClO^- at a concentration of 0.10 mmol L^{-1} for each anion, and $Cr_2O_7^{2-}$ at a concentration of 0.01 mmol L^{-1}) and the ion-exchange efficiency of $Cr_2O_7^{2-}$ was drastically decreased. The sample of **29** (or **30**) after ion-exchange was subjected to single-crystal X-ray diffraction, but only the structure of **29** containing the guest anions was obtained. It was observed that the $Cr_2O_7^{2-}$ anions fill into the channels to balance the framework charge, indicating that ion-exchange occurred exactly *via* a single-crystal to single-crystal process. Moreover, weak C–H···O interactions between the framework and $Cr_2O_7^{2-}$ anions were found. The phenomenon indicated that the anions, which need to go over very little resistance, are easily exchanged, and the large channels provide a fairly convenient passage for the diffusion of anions. These results can explain that **29** displays highly-efficient ion-exchange with excellent reversibility. More importantly, it demonstrates that the abovementioned adsorption capacity of Cr(VI) is correct because dichromate was identified as the principal component.[81]

Another example is the report that introduces an unprecedented 3D cationic MOF comprised of nanoscale cages composed of $[Ag_2(btr)_2]2ClO_4\cdot 3H_2O$ (**31**), which showed fast exchange, high trapping capacity, and good selectivity for the capture and separation of $Cr_2O_7^{2-}$ in water. Interestingly, the exchange of $Cr_2O_7^{2-}$ in **31** was performed *via* a single-crystal to single-crystal (SCSC) process. Given that a great deal of ClO_4^- was located in the voids of the framework of **31** and that enough large channels were available for anion access, anion exchange experiments were performed using $Cr_2O_7^{2-}$ as a model. When crystals of **31** were immersed in an aqueous solution of equimolar $K_2Cr_2O_7$, the $Cr_2O_7^{2-}$ concentration in the solution decreased by 37% and 60% after 1 h and 3 h, respectively. Subsequently, a slow decrease in the $Cr_2O_7^{2-}$ concentration was observed, and there were no evident changes in anion concentration and solution color between 24 h and 48 h. This emphasized that **31** has a superior performance for $Cr_2O_7^{2-}$ capture with fast exchange and high capacity. When they used double the molar amount of **31** with respect to $Cr_2O_7^{2-}$ under the same conditions, 66% and 90% of $Cr_2O_7^{2-}$ was exchanged after 0.5 h and 6 h, respectively. During the exchange, the solution changed from yellow to colorless. The $Cr_2O_7^{2-}$ capture ability was further investigated in more dilute aqueous solutions. As shown in their article, when an excess of **31** was placed in a 14.7 ppm aqueous solution of $K_2Cr_2O_7$, the crystals changed from colorless to yellow after 48 h. Their analysis indicated that the concentration of remnant $Cr_2O_7^{2-}$ was 0.09 ppm, suggesting the almost complete capture of $Cr_2O_7^{2-}$ (99.4%) by **31**. These results implied that **31** was a promising material for the removal of low-concentrations of $Cr_2O_7^{2-}$ from wastewater. In comparison with anion exchange, the anion selectivity may be more important and challenging. Selective exchange experiments were examined for mixtures of anions. When the crystals of **31** were immersed in an aqueous solution containing BF_4^-,

$CF_3SO_3^-$, NO_3^- and $Cr_2O_7^{2-}$ for 24 h, the crystals gradually turned yellow. In the IR spectrum of the resultant crystals, only the characteristic band arising from $Cr_2O_7^{2-}$ was observed, suggesting a good selectivity for $Cr_2O_7^{2-}$ over the other anions. The selectivity of **31** may be attributed to the stronger interactions of $Cr_2O_7^{2-}$ with the cationic framework in comparison with the other anions.[82]

Most MOFs are not stable in aqueous solutions and studies have shown that Zr-cluster based MOFs can be stable in aqueous solutions and are becoming promising candidates for pollutant elimination.[83,84] A cationic Zr-MOF, ZJU-101 (**32**), (prepared from a post-synthetic process of MOF-867, $Zr_6O_4(OH)_4\cdot(BPYDC)_6$ with trifluoromethanesulphonate) has been reported, which not only exhibits the highest $Cr_2O_7^{2-}$ removal capacity, but can also selectively remove $Cr_2O_7^{2-}$ from its aqueous solution within a very short period of time. **32** was synthesized from MOF-867 (ref. 85) through a post-synthetic modification, in which methyl groups were added to the pyridyl sites to form the cationic framework. In this study, the research group also compared the behavior of **32** with MOF-876. To evaluate and compare the adsorption activity of MOF-867 and **32**, anion exchange was performed by simply placing the dried adsorbent into a solution of dichromate and the solution was stirred under ambient conditions. According to the data, which are shown in the article, after 12 h, only a very small amount of dichromate (about 22%) was removed when MOF-867 was used as adsorbent. After the crystals of **32** were immersed in the aqueous solution of dichromate, the $Cr_2O_7^{2-}$ ion concentration decreased significantly by 87.8% in 5 minutes. After 10 minutes, over 96% of dichromate was removed from the aqueous solution. Apparently, **32** was superior to MOF-867 during the capture of $Cr_2O_7^{2-}$ ions. Once the dichromate was removed by **32** from the aqueous solution after 10 minutes, the solution became colorless after centrifugation. It was clear from the adsorption test that, for efficient anion exchange, the balanced ions within the pores of **32** made a significant contribution to the removal of dichromate. To further confirm the adsorption capacities of the MOFs towards dichromate, adsorption isotherms were collected for MOF-867 and **32** at room temperature. As the uptake was greatly influenced by the concentration of the $Cr_2O_7^{2-}$ solution, different concentrations of the $Cr_2O_7^{2-}$ solution were applied to determine the uptake. The overall adsorption capacity of **32** for the dichromate reached up to 245 mg g^{-1}, which was the highest among the porous materials used for dichromate removal reported to date. The uptake capacity of MOF-867 for dichromate was only 53.4 mg g^{-1}, which was significantly smaller than that of **32**. Given the high-capacity and fast ion-exchange function of **32**, the selective adsorption tests of **32** were also carried out for a variety of anions. The dried sample of **32** was immersed in a solution of $Cr_2O_7^{2-}$ together with *n*-fold molar excess of disturbing ions (*n* is equal to 0, 3, 6, 9 and 12) containing equal molar amounts of Cl^-, Br^-, NO_3^-, SO_4^{2-}, I^- and F^-. The results indicated that the adsorption capacity of **32** for $Cr_2O_7^{2-}$ was still as high as 88% when there was a 3-fold excess of disturbing ions. When there was a 12-fold excess of disturbing ions, the adsorption of $Cr_2O_7^{2-}$ was still at a high efficiency of 81%. The highly selective absorption was attributed to the strong columbic attractions between the framework and $Cr_2O_7^{2-}$, and the matching of $Cr_2O_7^{2-}$ with the pores.[86]

A three-dimensional water-stable cationic MOF pillared by a neutral ligand and with Ni^{II} metal nodes has been synthesized employing a rational design approach by A. V. Desai and co-workers. Due to the ordered arrangement of the uncoordinated tetrahedral sulfate (SO_4^{2-}) ions in the channels, the compound has been employed in aqueous-phase ion-exchange applications. This system is the first example of a MOF-based system that absorbs both dichromate ($Cr_2O_7^{2-}$) and permanganate (MnO_4^{2-}) ions. The water-stable, three-dimensional cationic MOF is $[\{Ni_2(Lig)_3\text{-}(SO_4)(H_2O)_3\}\cdot(SO_4)\cdot x(G)]_n$ (**33**), (G = H_2O and DMF), which was built from a tripodal neutral ligand and contains free sulfate ions. The guest-free phase of **33** acts as a fast and selective adsorbent for the capture of both monovalent and divalent tetrahedral oxo-anions, namely dichromate and permanganate ions (Fig. 9). They sought to harness the ionic functionality imparted by the cationic framework to investigate the anion exchange and loading properties of **33**. Due to the hydrolytic stability, robust 3D architecture, and channelized alignment of the free SO_4^{2-} ions, the ability of **33** to trap dichromate ions was investigated. Crystals of **33** were dipped into an aqueous solution of $K_2Cr_2O_7$ and the exchange process was monitored using different analysis methods. The partial decoloration of the solution and the change in color of the crystals showed the exchange of SO_4^{2-} ions with $Cr_2O_7^{2-}$. They believed that the anion exchange process lead to the occupation of the positions of the free sulfate ions (aligned in the porous channels) by $Cr_2O_7^{2-}$ ions. The group suggested that this swap was possible because one-half of the dichromate ion has a tetrahedron like geometry, even though the entire ion itself is not tetrahedral in shape. The other half of the dichromate anion could then reorganize itself in the free space as the anion position is directed towards the pore. In addition, to test

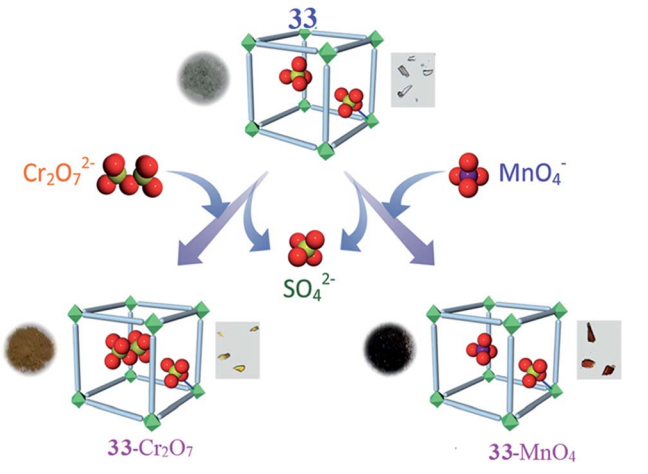

Fig. 9 A schematic representation of the capture of heavy-metal oxo-anions by **33** with the concurrent loss of SO_4^{2-} ions. Photographs of the different phases and crystals of the materials are shown with each representation. Reproduced with permission from ref. 87, copyright 2016, Wiley Online Library.

the selectivity of the system for dichromate capture, **33** was dipped into an aqueous mixture of $K_2Cr_2O_7$ and a salt of either ClO_4^-, NO_3^-, BF_4^- or $CF_3SO_3^-$ ions (separate experiments carried out for each ion). Careful analysis revealed that in all cases, $Cr_2O_7^{2-}$ was selectively incorporated inside the porous matrix over other competing anions. These results validated the hypothesis of employing tetrahedral exchangeable anions for the targeted capture of heavy metal oxo-anions. The uptake order was estimated to be as follows: $Cr_2O_7^{2-} > NO_3^- \sim ClO_4^- > BF_4^- > CF_3SO_3^-$. To check if **33** can function as a reversible absorbent, they attempted to desorb the loaded $Cr_2O_7^{2-}$ ions and replaced them with SO_4^{2-} ions. Although desorption was visible to the naked eye through color changes of both the supernatant and the solid, FTIR spectra suggested the replacement of dichromate ions with SO_4^{2-} ions. Furthermore, the desorbed phase of **33**-Cr_2O_7 could be used as a $Cr_2O_7^{2-}$ adsorbent, re-adsorbing the same amount of $Cr_2O_7^{2-}$ desorbed in the first cycle. Similarly, **33** was probed as an adsorbent for pertechnetate ion trapping by studying its response towards its congener: the permanganate anion. Crystals of **33** were dipped in an aqueous solution of $KMnO_4$ and the rapid decoloration of the solution with a simultaneous change in the color of the crystals from pale-green to dark-red was observed. Like in the case of $Cr_2O_7^{2-}$ exchange, almost a complete decoloration was noted after 72 h, giving rise to the exchanged phase **33**-MnO_4. The selective entrapment of MnO_4^- was explored by dipping **33** into an aqueous solution of $KMnO_4$ containing salts of either ClO_4^-, NO_3^-, BF_4^- or $CF_3SO_3^-$ ions. The FTIR spectra confirmed that competing anions were not included and suggested the selective uptake of permanganate ions. These results further confirmed the hypothesis that a tetrahedral substitutable anion acts as a facilitator for the capture of toxic-metal oxo-anions. An experiment to understand the preferential uptake between MnO_4^- and $Cr_2O_7^{2-}$ was undertaken by dipping **33**-Cr_2O_7 in an aqueous solution of $KMnO_4$ and separately by dipping **33**-MnO_4 in a solution of $K_2Cr_2O_7$. The results suggest that the framework had a higher affinity for MnO_4^- ions.[87]

3.1.2 Catalytic properties. Further studies in this field, have been carried out following the ion-exchange. S. Wang and coworkers reported a flexible porous MOF, $[Cu(II)(bped)_2(H_2O)_2(SiF_6)]I\cdot 4H_2O$ (Cu-MOF-SiF_6) (**34**) and its catalytic properties. Because **34** consists of 1D channels with SiF_6^{2-} hosted in the channels, an anion-exchange study was carried out. The SiF_6^{2-} can be readily exchanged with NO_3^- (**35**), while keeping the compound in a solution of NH_4NO_3. Both **34** and **35** were assessed for their catalytic activity in the selective oxidation of benzylic compounds to the corresponding carbonyl functionality.[88] To investigate the catalytic influence of anion-exchange, the oxidation of diphenylmethane catalyzed by **34** and **35** was investigated (Fig. 10a). The conversion to benzophenone was higher for **35** than **34** under similar conditions. The results showed that anion-exchange increases the catalytic activity of MOFs considerably.[89]

Heterogeneous catalysis has been investigated in this branch. In this prospect, reversible anion-exchange and the catalytic properties of two cationic MOFs based on Cu(I) and Ag(I) have been studied. The reported MOFs are SLUG-21 (**28**)

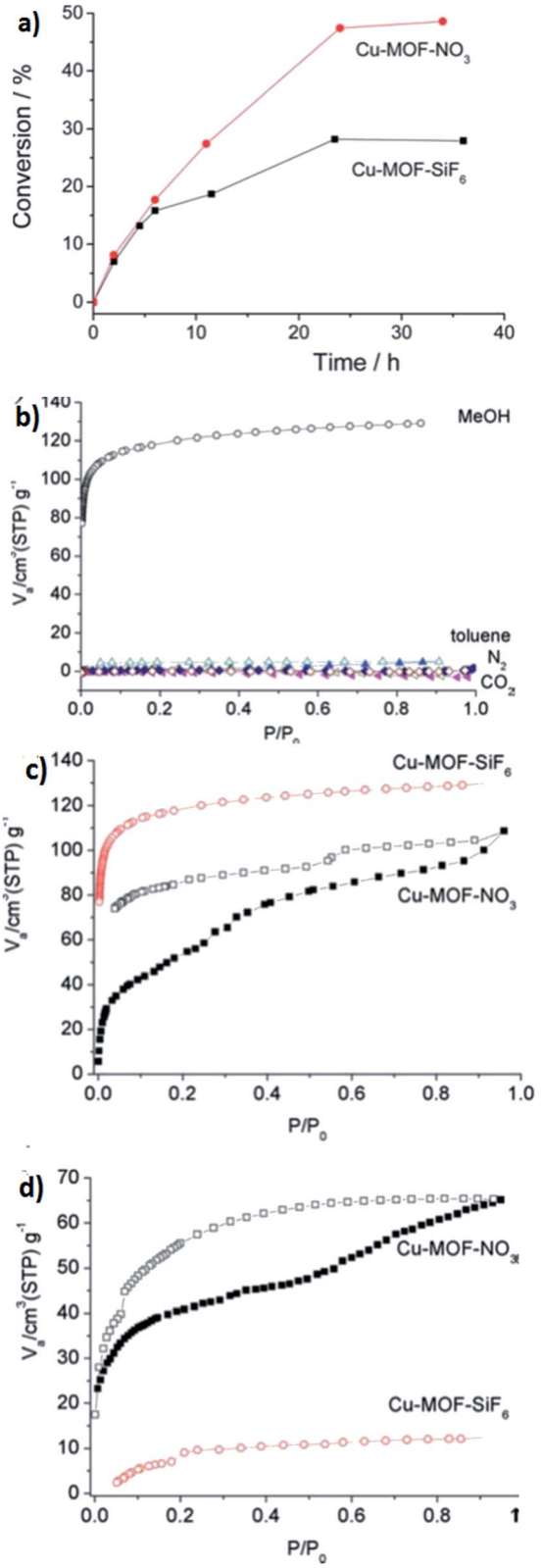

Fig. 10 (a) The kinetics of diphenylmethane oxidation catalyzed by Cu-MOF-SiF_6 (**34**) and Cu-MOF-NO_3 (**35**). (b) The N_2/CO_2 gas adsorption–desorption isotherms and MeOH–toluene vapor adsorption–desorption isotherms of $[Cu(II)(bped)_2(H_2O)_2(SiF_6)]I\cdot 4H_2O$. (c) MeOH and (d) EtOH vapor adsorption–desorption isotherms of $[Cu(II)(bped)_2(H_2O)_2(NO_3)]I\cdot 4H_2O$. Reproduced with permission from ref. 89, copyright 2011, Royal Society of Chemistry.

and SLUG-22 (**36**). Both of them show reversible anion-exchange between organosulfonate and various inorganic species. As primary examples of exchange, they have focused on several inorganic anions, such as the oxo-anions of several metals, nitrate and perchlorate. As a final example of pf anion-exchange capability, they investigated **28** for permanganate and perrhenate trapping. Compound **36** was also employed in the same exchange reaction with nitrate and perchlorate to gain insight into the structure–activity properties. Cationic MOFs are potentially useful for heterogeneous catalysis due to their positive charge compared to the majority of the reported MOFs. The group found that these two materials are catalytically active in heterogeneous ketal formation. Ketalization is an important method to support carbonyl groups in organic synthesis and drug design.[90] The reaction needs a Lewis acid catalyst to activate the oxygen of the carbonyl group, which permits glycol to replace the ketone group. Ketalization of 2-butanone, 2-pentanone and benzophenone by ethyl glycol was performed for both **28** and **36**.[91]

3.1.3 Adsorption properties. MOFs potentially have sorption isotherms due to their porosity. Sometimes they achieve new capabilities in adsorption after an exchange process; Cu-MOF-SiF_6 (**34**) has been introduced by F. X. L. Xamen *et al.* before to possess this ability. The MeOH adsorption/desorption isotherms of desolvated **34** are shown in Fig. 10b. Such an adsorption/desorption behavior clearly shows that **34** is flexible, making the solid able to adapt to the inclusion of MeOH guests. Interestingly, the physisorption isotherm of MeOH of the NO_3^--exchanged material is quite different from that of **34** (Fig. 10c). In comparison, the fast initial adsorption shows that **35** possessed intrinsic microporosity because the relatively smaller sized NO_3^- anions could not completely block the channels as found in the case of SiF_6^- anions. The EtOH physisorption of **34** and **35** (Fig. 10d) was somewhat similar to the MeOH uptake. The results suggest that anion-exchange changes the cavity size so that EtOH uptake is blocked for **34** but allowed for **35**.[88]

3.1.4 Luminescent properties. The luminescent properties have also been studied for exchanged MOFs. One of the reported MOFs with a cationic framework is $[Ln(TTP)_2]\cdot(CF_3SO_3)_3\cdot C_3H_6O\cdot 5H_2O$ (Ln = Eu for **37** and Ln = Gd for **38**). Anion-exchange of CF_3^- by smaller ClO_4^- and SCN^- was investigated. The luminescent spectra were recorded for the Eu^{3+} complex in the solid state. The anion-exchange and luminescent studies displayed the important potential of using such highly connected lanthanide MOFs as porous and optical materials.[92]

Luminescent cationic MOFs with extra-framework anions suggest a dynamic framework and tunable luminescent behavior by exchanging these framework anions with other anions of different shape, size and coordination nature. The luminescent behavior of $[\{Zn(L)(MeOH)_2\}\text{-}(NO_3)_2\cdot xG]_n$ (**39**) (in which G are disordered guest molecules and the linear bichelating ligand L was synthesized by Schiff-base condensation of 4,4′-ethylenedianiline and 2-pyridine-carboxaldehyde in high yield) has been investigated. The 1D channel of the compound was filled with NO_3^- anions. Anion-exchange experiments using anions with a weak or non-coordinating nature, such as ClO_4^- and $N(CN)_2^-$ (type A), and anions with a strong coordinating nature, such as N_3^- and SCN^- (type B), were performed. The framework can easily adjust its channel dimension to encapsulate different guest anions because of its dynamic nature. The anion selectivity experiments show that the order of association of guest anions to the framework was $SCN^- > N_3^- > N(CN)_2^- > ClO_4^-$ (Fig. 11a).

The anion-exchanged materials demonstrated amazing anion-dependent luminescent behavior (Fig. 11b). As a result for the anion-exchanged compounds of type A, a high enhancement of fluorescence was observed and on the other hand, for the anion-exchange compounds of type B, fluorescence quenching was observed.[93]

Compound **27** was introduced by P. F. Shi *et al.* previously, which acted as a luminescent probe. To further study the effect of $Cr_2O_7^{2-}$ on the luminescence of **27**, solid-state photoluminescent spectra were obtained. The typical luminescence peaks of Dy^{3+} in **27** were observed at 479 and 573 nm. With $Cr_2O_7^{2-}$ continuously entering into the channels, the luminescent intensity dropped rapidly, originating from the fact that the electron transfer transitions of $Cr_2O_7^{2-}$ decreased the energy transfer from $BPDC^{2-}$ to Dy^{3+}. However, upon the

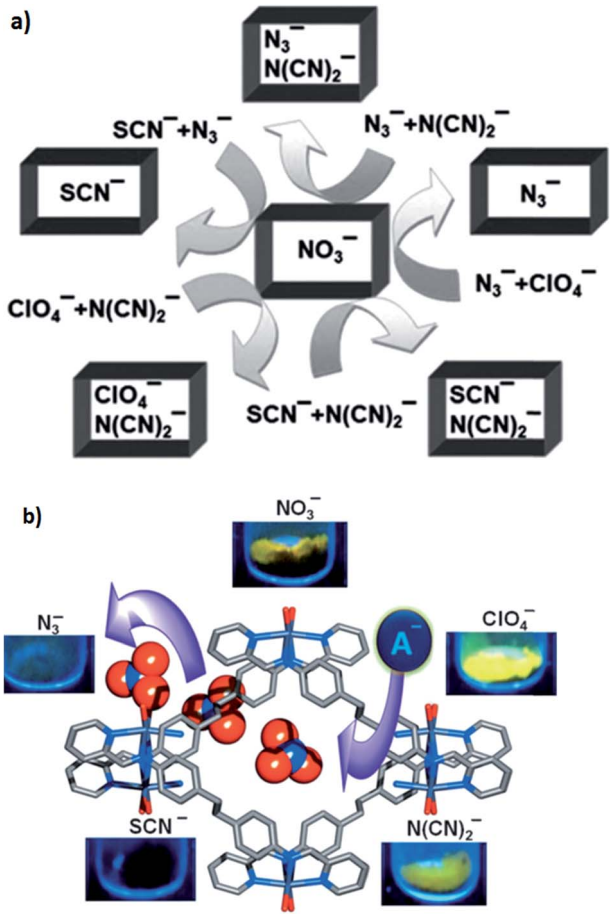

Fig. 11 (a) A schematic representation of the anion selectivity with the combination of two anions in $[\{Zn(L)(MeOH)_2\}\text{-}(NO_3)_2\cdot xG]_n$. (b) The effects of anion-exchange on the luminescence properties of $[\{Zn(L)(MeOH)_2\}\text{-}(NO_3)_2\cdot xG]_n$ (**39**). Reproduced with permission from ref. 93, copyright 2013, John Wiley & Sons.

sample containing $Cr_2O_7^{2-}$ being immersed in a solution of Na_2SO_4 or K_2CO_3, the intensity may have significantly rebounded with the release of $Cr_2O_7^{2-}$ upon exchange with SO_4^{2-} or CO_3^{2-}, which elucidated the capture and release process of $Cr_2O_7^{2-}$. Thus, **27** may be considered as a luminescent probe of $Cr_2O_7^{2-}$.[78] The effect of anion-exchange on the luminescence properties was also explored using compound **31**. **31** emitted a blue-violet light under UV irradiation, whereas the **31**·Cr_2O_7 emission was almost invisible to the naked eye. The solid-state emission spectrum of **31** at room temperature displayed a broad emission band centered at 450 nm upon excitation at 345 nm, a value that was in agreement with the emission observed under UV irradiation. The emission may be attributed to ligand-to-metal charge transfer (LMCT) transition.[94] However, the luminescent emission was largely suppressed after the exchange of ClO_4^- with $Cr_2O_7^{2-}$. The disappearance of the luminescent emission in **31** was probably because the electron-transfer transitions of $Cr_2O_7^{2-}$ decreased the energy transfer from the btr ligand to Ag^I. Thus, **31** is considered as a luminescent probe for $Cr_2O_7^{2-}$.[82]

3.1.5 Other applications. Studying the magnetic properties is one of the issues that has been noticed. In this aspect, [Ln(bipyNO$_4$)](Tfo)$_3$·x·solvent (Ln = Tb, Dy, Ho, Er) (**40**) is presented. As we know, the incorporation of new species into the pores of MOFs is one of its main applications. The $[TfO]^-$ anions are effectively exchanged with POM^- accompanied by a color change of the crystals from colorless to yellow. Importantly, the structural features of the network remain unchanged upon anion-exchange. More interesting is the observation that the slow magnetic relaxation is preserved after POM incorporation. Finally, in the interest of these magnetic frameworks in molecular magnetism, the scattering of the POMs inside the big cavities, prepared by this porous structure, leads to solids in which the POMs present an extraordinary surface area.[95]

In another case, the first example of highly efficient iodine enrichment based on a Cd(II)-triazole MOF *via* an ion-exchange approach was reported. The report was about [Cd(4-amino)$_2$(-ClO$_4$)$_2$]·H$_2$O (**41**) and its anion-exchange approaches. The experiments indicate that the original ClO_4^- anions are replaced by I_3^-. For detection of the enrichment of IO_3^- in dilute solution by anion-exchange based on the MOF, the crystals of **41** were dipped in an aqueous solution of $NaIO_3$.[96]

3.2 Applications of the cation-exchange process

3.2.1 Separation of gases. Cation-exchange of an anionic metal organic framework can also have some effects and applications that have been investigated here in different branches by us. Elsa. Q and co-workers reported an anionic MOF, NH_4[Cu$_3$-(μ_3-OH)(μ_3-4-cpy)$_3$] (NH_4@1) (**42**) and studied its cation-exchange and related complications. They examined the exchangeable nature of the extra framework NH_4^+ cations as a way to modulate the porous structure of this material. During their experiments NH_4^+ ions could be replaced by Li^+, Na^+, K^+, Ca^{2+}/2, La^{3+}/3, Et_3NH^+ and Me_3NH^+. The results showed that the ion-exchange processes on these systems lead to profound changes in the textural properties of their porous surface and in the adsorption selectivity of different separation processes of gases and vapors. The N_2 adsorption measurements performed on the exchanged systems show profound changes in the adsorption isotherms concomitant to the ion-exchange processes, which are indicative of the modulation of the porosity of **42**. Indeed, on passing from NH_4^+ to Et_3NH^+ a reduction in the adsorption capacity and pore surface was observed. They also tested the effect of the ion-exchange processes on the separation selectivity by adsorption of gases such as N_2, CH_4, CO_2, C_2H_2 and harmful vapors (benzene, cyclohexane). CO_2/C_2H_2 as well as benzene/cyclohexane mixtures are difficult to separate as a consequence of their similar physical properties, and thus it is of interest to find methods for their efficient separation. They showed the possible utility of this type of microporous network for the separation of C_2H_2/CO_2. Variable-temperature pulse gas chromatography experiments were carried out in the 273–363 K temperature range with a complex gas mixture (N_2, CH_4, CO_2, and C_2H_2) to examine the possible utilization of these systems for gas separation purposes. The results show that the A@**42** (A = NH_4^+, Et_3NH^+) frameworks give rise to significant interactions with acetylene and carbon dioxide, whereas the interactions with nitrogen and methane are negligible.

Notably, at low temperatures (T < 286 K), acetylene was more tightly retained by the A@**42** frameworks compared with carbon dioxide. At higher temperatures (T > 286 K) the reverse situation was found, with C_2H_2 being eluted before CO_2. They also studied the effect of ion-exchange on the separation selectivity towards benzene/cyclohexane mixtures. In the case of the original NH_4@**42** sample, the composition of the adsorbed benzene/cyclohexane phase reaches a 5 : 1 ratio, already showing a clear enrichment in the benzene component. This is further substantiated in the case of the Et_3NH@**42** and Li@**42** materials with benzene/cyclohexane ratios of 8 : 1 and 12 : 1, respectively. The increased selectivity of the Et_3NH@**42** and Li@**42** systems is related to the increasing bulk of the Et_3NH^+ and $Li(H_2O)_4^+$ ions.[97]

As the next example, an anionic nanoporous framework material with mobile guest cations [HDMA]$_3$[(Cu$_4$Cl)$_3$-(btc)$_8$]·9DMA (**43**) has been reported. This MOF can perform ion-exchange with tetraalkylammonium cations, such as TMA (**44**), TEA (**45**) or TPA (**46**). The research group also indicated that cation-exchange within this anionic framework creates unusual pore partition effects on gas separation (CO_2/N_2). The results revealed that **46** with the smallest pores and volumes may be better suited for separating CO_2 over N_2 and showed the highest selectivity of 106.8 during CO_2/N_2 adsorption. Finally, they reached the conclusion that ion-exchange using organic cations to tune the pore space for gas separation is a promising course for the improvement of new functional MOFs materials.[98]

3.2.2 Catalytic properties. The catalytic properties of anionic MOFs are another aspect that has been regarded after the exchange processes. Y. Tan and co-workers presented an unusual microporous MOF, namely [Zn$_{17}$thb$_{14}$(μ_4-O)$_4$(H$_2$-O)(HDMA)]·Me$_2$NH$_2$·xguest (**47**). The compound can perform ion-exchange with Pd^{2+} (**48**) or Ag^+ (**49**) cations and can also

reduce them into Pd or Ag-NPs in its pores upon heating. During the exchange process, the guest $Me_2NH_2^+$ cations in CH_2Cl_2 exchanged sample of MOF can perform ion-exchange with Pd^+ or Ag^+ cations. The interesting aspect of this study was the observation of a thermally-driven charge from the anionic host to the guest cations, which leads to the direct preparation of M-NPs inside the pores of a MOF. Furthermore, the catalytic properties of **48** and **49** were examined as a hydrogenation catalyst that led to a complete and fast conversion of styrene to ethylbenzene. However, **49** had a very low activity in the reaction system and gave low conversions. The results showed that catalyst **48** could be reused several times without reducing the activity.[99]

Another study described the heterogenization of single site transition-metal catalysts in MOFs *via* cation-exchange. Their efforts focused on the exchange of endogenous $HDMA^+$ cations with cationic transition-metal complexes in anionic $(HDMA)_3[In_3(BTB)_4]\cdot 12DMF\cdot 22H_2O$ (ZJU_28) (Fig. 12) (**50**). Furthermore, the Rh-containing MOF **50** was shown to be a recyclable catalyst for alkene hydrogenation and demonstrated developed catalytic performance related to its homogeneous counterpart under certain conditions.[100]

An anionic MOF, $[HDMA]_2[Zn_2(BDC)_3(DMA)_2]\cdot 6DMF$ (**51**), has been investigated in several studies to date because of its cation-exchange ability and subsequent applications. We will discuss this MOF in the following sections, but here we discuss the results of its catalytic properties. The prepared MOF has an anionic framework with $[HDMA^+]$ cations in the channels. These cations are exchanged with Ni^{2+} (**52**), Na^+ (**53**), Li^+ (**54**), (TEA^+) (**55**) and $(TPA)^+$ (**56**) during the experiments. Using this strategy, they were able to prepare cation-exchanged anionic MOFs as a novel heterogeneous catalytic system for the solvent-free Knoevenagel condensation reaction between benzaldehyde and malononitrile. The catalytic activity of the compound **51** apohost framework was studied. They thought that the catalytic activity of **51** was as a result of its anionic framework. Thus, in order to examine this idea, the activated samples of **52**, **53** and **54** after the post-synthetic exchange were studied too. The obtained results showed that the catalytic activity decreased in the order of **51** > **54** > **53** > **52**. As it was clear, the ionization potential decreased in the following order: $Ni^{2+} > Li^+ > Na^+ > HDMA^+$. Therefore, by increasing the ionization potential of the cations in the channels of **51**, the acidic properties of the metal ions increased and the basic properties of the anionic framework decreased. In order to confirm this supposition, they performed cation-exchange processes of $HDMA^+$ with the larger organic cations of **55** and **56**. The experiment proved this hypothesis too and indicated that the catalytic activities decreased in the order of **56** > **55** > **51**. Consequently, they showed that with a simple post-synthetic cation-exchange in anionic MOFs, some new solids with different catalytic activities were produced.[101]

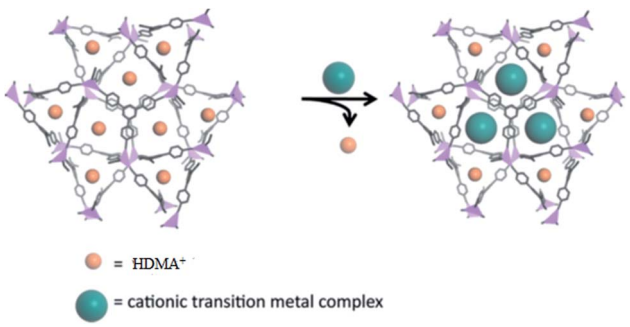

Fig. 12 The proposed heterogenization of single-site transition-metal catalysts in ZJU-28 (**50**) *via* cation-exchange. Reproduced with permission from ref. 100, copyright 2013, American Chemical Society.

In this section, another novel application of these anionic MOFs as heterogenous catalysts is introduced. S. Beheshti *et al.* were able to prepare a cation-exchanged anionic MOF as a new heterogeneous catalytic system for the solvent-free Micheal addition of pyrrole to electron-deficient β-nitro styrenes. In this case, using cation-exchange as post-modification in the anionic MOF, $[HDMA]_2[Zn_2(BDC)_3(DMA)_2]\cdot 6DMF$ (**51**), the catalytic activity was improved. The $[HDMA^+]$ cations in MOF were replaced with $(TEA)^+$ (**55**) or $(TPA)^+$ (**56**) *via* cation-exchange. The catalytic activity of the compound **51** apohost framework was studied in the Micheal addition reaction. They attributed the activity of **51** to its anionic framework. Thus, in order to approve this hypothesis, activated samples of **55** and **56** were used after post-synthetic cation-exchange. The results of applying the apohost frameworks of **55** and **56** in the Micheal reaction confirmed this idea and indicated that the catalytic activity decreased in order of **56** > **55** > **51**.[102]

3.2.3 Gas adsorption. Subsequently, the ion-exchange processes of different MOFs can achieve new abilities in the adsorption of various gases.

Hydrogen adsorption. As we have insinuated, ZMOFs are anionic and have readily exchangeable extra framework cations. F. Nouar and co-workers showed that ZMOFs can be regarded as a platform for systematic studies on the effect of different structural factors on H_2 interactions with porous metal organic materials. In their study, $|(HPP^{2+})_{24}|[In_{48}(HImDC)_{96}]$ (HPP-*rho*-ZMOF) (**57**) was reported as the parent framework, where the Na^+ ions replaced the extra-framework cations. The group reported the effect of several extra-framework cations ($HDMA^+$, Li^+, Mg^{2+}) on the H_2 sorption energetics and uptake. Li^+ cations have a small ionic radius compared to most inorganic cations; this results in a reduced framework density and large enough voids for H_2 storage. The other cation, Mg^{2+}, is also ionized because of its high dependency for H_2. The Li^+-exchanged material, Li-rho-MOF (**58**), can store slightly more H_2 molecules per In. It is important to note that the slightly higher value for **58** is in contrast to results obtained in the previous Li^+-exchanged MOFs, which show no proof for strong H_2–Li^+ interactions.[103]

A more detail study has been carried out in this case. Herein, they illustrated a systematic study of the solvothermal conditions used for optimizing the synthesis of the two mentioned ZMOF structures (Rho (**59**) and Sod (**60**)). Both the Rho and Sod ZMOF materials were prepared basically following the procedure published elsewhere, in which (H_3ImDC), $In(NO_3)_3\cdot XH_2O$, (DMF), CH_3CN, (HPP), and HNO_3 were consecutively added to obtain a mixture. These materials were exchanged with Li^+, Na^+, K^+ and Cs^+ cations. The H_2 sorption of the as-prepared and

exchanged materials was discussed too. The ion-exchange degree of these three cations (Na^+, K^+, Li^+) in **60** were measured. The results showed that the ion-exchange degree increased with the cation size. In regard to the H_2 adsorption, their experiments show that Na^+Me-sod ZMOF adsorbs less H_2 than the non-exchanged sod-ZMOF, although the exchanged material has a higher surface area. This behavior suggests that the weaker adsorption of H_2 by Na^+ can be compensated by its smaller cation size, which results in a higher surface area and pore volume of the exchanged material. In comparison with the sample exchanged only once with Na^+, the sample exchanged four continuous times with Li^+ showed very similar results with H_2 uptake. The K^+-exchanged sample was not crystalline enough to extract any conclusion about its association for H_2.[104]

Enhancement of the isosteric heat of adsorption for H_2 in the Li-exchanged rho-ZMOF is an interesting instance that has been investigated by S. Yang and co-workers. Synthesis of three anionic frameworks (NOTT-206-solv) (**61**), (NOTT-200-solv) (**62**) and (NOTT-208-solv) (**63**), and their organic cation replacement with Li^+ (NOTT-209-solv) (**64**) have been reported. Both **63** and **64** showed reversible H_2 sorption isotherms, which are consistent with their larger pores. Furthermore, they reported that **63** and **64** have identical framework structures, the enhancement in the H_2 storage capacities can be linked to the cations, H_2PPZ^{2+} or Li^+, animating in the channels. Their findings indicate that the gas storage properties of the charged MOFs are controllable by the choice of the counter-ions; different cations within the pores may act as a code for the enhancement of H_2 storage properties.[105]

The other description was about an anionic MOF material built from In(III) centers and H_4L ligands. The framework presented hysteretic hydrogen adsorption with piperazinium $(H_2PPZ)^{2+}$ dications in its pores. The paper demonstrated the synthesis of 1-PPZ-solv MOF (**65**) and its exchange reaction product, Li-PPZ-solv (**66**). During the exchange, the H_2PPZ^{2+} dications were replaced by Li^+ (Fig. 13). The MOF **65** showed a considerable kinetic trap (hysteresis) for H_2 and N_2 adsorption, whereas **66** showed an increase in both pore volume and a notably higher isosteric heat of adsorption for H_2 compared with **65**. Their results exhibited a cation-dependent hysteretic H_2 sorption with the hysteresis tunable by post-synthetic modification *via* cation-exchange.[106]

Do-MOF (**67**) was introduced by K. Mulfort *et al.* The combination of an octa-oxygen ligand with a Zn(II) source and the diol-containing strut, after two days of heating, results into colorless block crystals of **67**. Do-MOF is a non-catanated hydroxyl functionalized MOF and exchange of the hydroxyl protons for Li^+ and Mg^{2+} cations was investigated. The replacement of Li^+ by a more highly charged cation may increase the heat of adsorption, and therefore they also examined an Mg^{2+} containing version. In this study, the H_2 uptake was also measured and its diminution after the exchange was reported. In their experiments, the low-pressure adsorption of H_2 by **67** was reversible at 77 K and reached 1.23 wt% at 1 atm. **67**-Li exhibited only a slightly greater uptake (1.32 wt% at 1 atm). Nevertheless, the increase corresponds to two additional H_2 per Li^+. Their finding was broadly consistent with computational predictions that an exposed lithium cation on carbon or MOF materials can (depending on pressure) directly bind up to six H_2 molecules.[107]

In the bunch of ZMOFs that have adsorption properties, another ZMOF has been reported. $([In_{80}(Himdc)_{160}]^{80-})_n$ (Usf-ZMOF) (**68**) was introduced by Y. Liu, *et al.* The anionic character, extra-large cavities, large openings and chemical stability in an aqueous solution of Usf-ZMOF allowed the full exchange of the 1,2-H_2DACH cations with different organic and inorganic cations, including Li^+, Na^+ and Mg^{2+}. In order to detect the gas sorption properties of **68**, the extra framework cations present in the as-synthesized compound were fully exchanged with DMA cations. Gas sorption experiments were performed on DMA-exchanged **68** and the fully evacuated framework exhibited permanent microporosity. H_2 sorption studies were also performed and the results showed a relatively enhanced isosteric heat of sorption at lower loadings that can be related to the charge nature of the cavities.[108]

We have already discussed the gas separation of $[HDMA^+]_3[(Cu_4Cl)_3\text{-}(btc)_8]\cdot 9DMA$ (**43**). Another application of this MOF that has been reported after ion exchange is gas adsorption. Cation-exchange within the anionic framework created unusual pore partition effects on the gas adsorption (N_2, CO_2 or H_2). The H_2 adsorption observed for the MOF and exchanged-MOF was measured. The authors noted that the H_2 adsorptive dependence on the framework was not just concerned with the surface area, but was also concerned with the suitable pore volume.[98]

The last example, examined by us, was the MOF materials $\{(A)[In(L^n)]\cdot solv\}_\infty$, (A = $1/2H_2PPZ^{2+}$ or $HDMA^+$, solv = DMF, CH_3CN and H_2O) (**69**) that have been prepared from In(III) with tetracarboxylate isophtalate-based ligands. The MOFs were comprised of organic cations, H_2PPZ^{2+} or $Me_2NH_2^+$. The organic cations within the as-synthesized materials could be exchanged with Li^+ ions (Fig. 14). The gas adsorption of H_2 and N_2 has been studied in detail. Thus, an increase in the H_2 capacity and overall porosity were observed on going from the desolvated MOF incorporating $HDMA^+$ cations to desolvated MOF incorporating Li^+. They also demonstrated that by varying the pore gate and the isophthalate-based bridging ligand, the desolvated framework materials display either non-porous, or hysteretic, or reversible N_2 sorption properties, respectively. The group thus reported that the desolvated Li^+-exchanged framework materials did not show adsorption/desorption hysteresis with H_2,

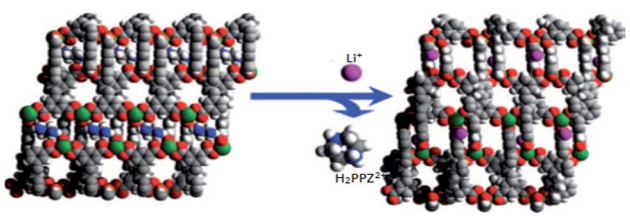

Fig. 13 Views of framework structures of 1-PPZ-solv (**65**) and Li-PPZ-solv (**66**). The H_2ppz^{2+} dications in channel B of **65** can be completely exchanged with Li^+ ions in channel C of **66**. Reproduced with permission from ref. 106, copyright 2009, Nature publishing group.

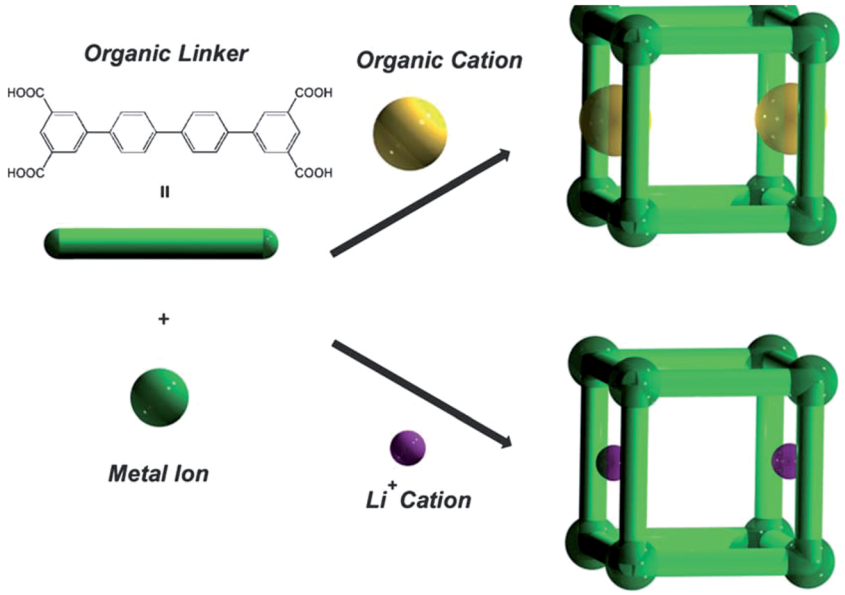

Fig. 14 A schematic representation of the construction of modulated MOFs in $\{(A)[In(L^n)]\cdot solv\}_\infty$ (**69**) with different pore gates. Reproduced with permission from ref. 109, copyright 2011, Royal Society of Chemistry.

but enhanced H_2 adsorption properties in terms of both the valencies and adsorption enthalpies.[109]

Carbon dioxide adsorption. The CO_2 adsorption properties are another application considered *via* cation-exchange. Our studied paper is about Bio-MOF, $Zn_8(ad)_4(BPDC)_6 0.2HDMA$ (**70**) and the replacement of its $HDMA^+$ cations with other organic cations such as TMA, TEA and TBA. The researchers also demonstrated that the post-synthetic exchange of the extra framework cations within the anionic Bio-MOF-1 can be used as a means to systematically modify its pore dimension and metrics. They efficiently used this strategy to optimize its CO_2 adsorption properties. To determine the effects of the pore modifications on the CO_2 capacity of this MOF, they studied the CO_2 adsorption of **70** and the exchanged MOFs. They interestingly animadverted on the contemplation that the CO_2 capacity of the MOFs did not depend on the pore volume and BET surface area. At all the temperatures studied, compound **70** showed the lowest CO_2 capacity compared to the exchanged-MOFs. They found that TEA@**70** had the largest CO_2 capacity at each temperature and TBA@**70** was nearly as effective as TMA@**70**. It was notable that TBA@**70** was a more effective CO_2 sorbent than **70**, even though its pore volume and surface area were almost half as large.[110]

In the group of ZMOFs, CO_2 adsorption has been obtained for the Sod topologies only. A research group that published their results in this case, reported that ion-exchanged sod-ZMOFs (**71**) by alkali-metals resulted in improved CO_2 adsorption performance compared with the as-prepared ZMOF. In this study, ion-exchange of **71** by different alkali metals such as Li^+, Na^+, K^+ and Cs^+ cations was carried out to study the effects of ion-exchange alkali metal on CO_2 adsorption. As a result of their experiments, they reported that all the ion-exchanged **71** samples displayed improved CO_2 adsorption capacity over the as-prepared sample. The highest CO_2 capacity was achieved by K^+-sod-ZMOF (**72**). They concluded that the CO_2 adsorption capacity in ion-exchanged sod-ZMOF appeared to depend not only on the size and charge of the balancing cations, but also on the dispensation of the cations located in the framework structures.[111]

Nitrogen adsorption. NOTT MOFs including NOTT-206-solv (**61**), NOTT-200-solv (**62**) and NOTT-208-solv (**63**) and their Li^+-containing framework (**64**) were discussed in the previous section on H_2 adsorption. N_2 adsorption has been also considered using these materials. By replacing the $HDMA^+$ cations with Li^+ ions, both of the channels released and accordingly, the adsorption of N_2 in NOTT-207 showed a typical type-I isotherm with little hysteresis. Therefore, using a combination of Li^+ with NOTT-207, the internal surface area became fully available for N_2 uptake. Modulation of the gas adsorption properties with different pore gates in NOTT-MOF materials has been finally demonstrated (Fig. 15).[105]

Another MOF that has been introduced and explicated N_2 adsorption is compound **34**. We have previously discussed its gas separation properties and the gas adsorption application of this MOF is now considered. In the mentioned study, N_2 adsorption measurements were performed on the exchanged systems and the results showed changes in the adsorption isotherms due to the ion-exchange processes. Indeed on going from NH_4^+ to Et_3NH^+, a lowering of the adsorption capacity and pore surface was observed.[97]

Some novel synthesized ZMOFs, such as sod-ZMOF derived from 4,6-PmDc $[In\text{-}(C_6N_2O_4H_2)_2Na_{0.36}K_{1.28}](NO_3)_{0.64}(H_2O)_{2.1}$ (**73**), also possess this property. The reaction between 4,6-PmDC and $In(NO_3)_3\cdot 5H_2O$ in a solution of DMF and water afforded pale yellow homogeneous crystals with polyhedral morphology, referred to as sod-ZMOF. Complete exchange of the K^+ cations

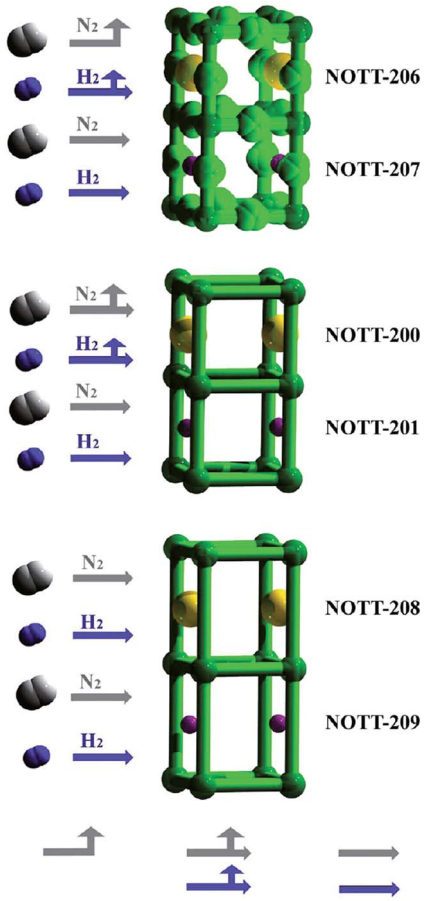

Fig. 15 Modulation of the adsorption properties with different pore gates in NOTT-MOFs. Reproduced with permission from ref. 105, copyright 2011, American Chemical Society.

with smaller Li^+ cations in this ZMOF was demonstrated. In addition, gas adsorption experiments were performed on the Li^+-exchanged sample. The result of the experiments demonstrated that the Li^+-exchanged and fully depleted sod-ZMOF, displaying permanent microporosity, as evidenced by the reversible type I N_2 and Ar adsorption isotherms. The dual character of ZMOFs, anionic frameworks and/or containing large accessible cavities, forms a suitable platform to evaluate the effect of pore size and/or intra-/extra framework charge density on the hydrogen uptake and its sorption energetics. Accordingly, hydrogen sorption studies were conducted on both compounds at 78 and 87 K at atmospheric pressure using this compound **73**.[112]

A zinc-based MOF $\{(HDMA)_2[Zn_3(BDC)_4]\cdot DMF\cdot H_2O\}$ (**74**) was synthesized by a research group and its cation-exchange processes and N_2 adsorption isotherms have been investigated. In order to study the cation-exchange process in a crystal-to-crystal transformation, initially they examined the stability of the compound's crystallinity in various solvents; however, the MOF only retained its crystallinity in DMF. A post-synthetic cation-exchange process of the MOF was carried out using Cu^{2+} (**75**), Li^+ (**76**) and Na^+ (**77**). During the exchange, $HDMA^+$ cations were replaced by Cu^{2+}, Li^+ and Na^+. The sorption properties of **74** were investigated using N_2 adsorption isotherms. They reported that compound **74** showed a typical type V adsorption curve and also mentioned that this strange behavior can be attributed to the blocked channels of **74** by the large, non-removable $HDMA^+$ cations.[113] A comparison of the N_2 isotherms obtained for compound **74** and **76** show a change in the adsorption isotherm from type V in compound **74** to type I in compound **76**. This behavior was because of the existence of small Li^+ cations in the channels of **76**, which were not an impediment for entrance of N_2 molecules compared with the blocked channels in **74** by the large, non-removable $HDMA^+$ cations. Thus compound **76** showed type I adsorption, indeed the channels of **74** only opened at high pressure of N_2 gas.[114]

A solid-type MOF constructed from heterometallic alkali metal is the last example that will be described by us in the N_2 adsorption area. The obtained MOFs were $[(CH_3)_3NH][NaVO(BTC)_{4/3}]\cdot 0.5DMF$ (**78**) and $\{[(CH_3)_4N]_3LiVO(BTC)_2\}$ (**79**), which represent the first MOF constructed from V/alkali metal mixed metal-oxo clusters. The effective free volumes of these compounds and their high architectural stability actuated the research group to follow cation-exchange experiments. The organic amine cations within the channels can be replaced by transition metal ions through a cation-exchange process. The Cu(II) ion was used as a suitable probe for the exchange experiments considering its size, stability and instinct. An N_2 adsorption measurement was subsequently carried out for the fully activated sample of sod-ZMOF, which was achieved by dipping the crystals in Cu^{2+} ion-containing acetone for 12 h, followed by heating at 80 °C for 12 h in a vacuum. The N_2 sorption isotherm reveals characteristic type II behavior. The analysis of the isotherm revealed a specific surface area S_{BET} = 122.5 $m^2\ g^{-1}$ (Langmuir, 196.4 $m^2\ g^{-1}$). A maximum N_2 uptake of 101 $m^2\ g^{-1}$ (at standard temperature and pressure, STP) was reached at 1 atm. They also measured the gas adsorption isotherms of fresh samples of **78** using the same method. However, the maximum N_2 uptake was very small at STP as the guest amine cations reside in the frameworks and the amine cations could not be removed with the neutral solvent. An analogous N_2 adsorption measurement was carried out for compound **79**. The analysis of the isotherm revealed a specific surface area S_{BET} = 316 $m^2\ g^{-1}$ (Langmuir, 368 $m^2\ g^{-1}$). A maximum N_2 uptake of 129 $m^2\ g^{-1}$ (at STP) was reached at 1 atm.[115]

Methane adsorption. Although, the physical adsorption of methane on MOFs has amused much interest, limited achievement has been obtained in storing methane under ambient conditions. The only in depth study on methane storage in anionic MOFs *via* cation-exchange was carried out by K. Akhbari *et al.* Their study started from post-synthesis cation-exchange of $[HDMA]_2$-$[Zn_2(BDC)_3(DMA)_2]\cdot 6DMF$ (**51**). We discussed this MOF in the Catalytic properties section. Herein, the CH_4 adsorption properties were considered. The existence of $HDMA^+$ organic cations in the channels of the MOF with an anionic framework established the possibility of their post-synthetic cation-exchange with metal ions such as Ni^{2+} (**52**), Na^+ (**53**), Li^+ (**54**), Cu^{2+} (**80**) and K^+ (**81**). The methane adsorption capacities of all of these materials were also measured. The

results showed an increase in the CH_4 adsorption capacity going from **51** to the last MOF (**81**), and Li^+-exchanged MOF (**54**) with the highest surface area had the highest methane adsorption capacity. Nevertheless, it was noted, by post-synthetic cation-exchange of **51** with some metal ions and particularly with Li^+, that we can successfully modulate the surface area and methane adsorption capacity. Another interesting result was reported that K^+-exchanged MOF (**81**) did not have any available pores for the adsorption of methane. On the other hand, the lowest N_2 gas sorption in **51** and the same surface area of **51** and **81** indicated that the MOF material of **51** did not allow N_2 gas molecules to enter its channels, but the channels in **51** showed different behavior upon facing methane gas molecules and showed a low CH_4 adsorption capacity. Therefore, the $HDMA^+$ cations in **51** act as a gate in an opposite way to N_2 gas molecules, permitting the CH_4 gas molecules to enter their channels.[116]

Other materials adsorption. The adsorption of volatile organic compounds in porous MOFs is one of the studied cases that was not comprised in the different gases group. Accordingly, F. J. Ma *et al.* achieved the functionalization of MOF (NENU-3) (**82**) with (Cu_3(BTC)$_2$) frameworks and POMs. They further modified the inclusion state of these materials *via* ion-exchange. A complete exchange of $(CH_3)_4N^+$ by K^+ was observed without losing the MOF structure (NENU-28) (**83**). For the VOCs adsorption studies, they selected methanol, ethanol, 1-propanol, 2-propanol, cyclohexane, benzene and toluene. The adsorption isotherms of methanol showed a corresponding development in the storage capacity on **83**. By continuing their experiments, they found that the exchange of alkali metal cations may also bring on an increase in the adsorption capacity when comparing the data of **82**. The results of the Li^+-exchanged MOF (**84**) also confirmed their deduction. Alkali metal exchanged **82** and **84** bring an extra interaction with the adsorbed molecules, which leads to a significant enhancement in adsorption. At the end of the study, it was reported that **83** displays the best adsorption for VOCs. In addition, the data obtained from N_2 adsorption studies were also reported in their work, and an increasing adsorption capacity of **82** upon K^+-exchange was suggested.[117]

The selective adsorption of dyes *via* ion-exchange is also notable. In this case, IFMC-2 $[HDMA]_4[(Zn_4dttz_6)Zn_3]\cdot 15DMF\cdot 4.5H_2O$ (**85**) has been used. The Ln(III)-loaded MOF material Ln^{3+}@**85** and the adsorption of cationic dyes through ion-exchange were also investigated. IFMC-2 (**85**) has an anionic framework, which is filled with $[HDMA]^+$ ions and guest molecules. The $[HDMA]^+$ ions can be exchanged with Ln^{3+} cations. The organic cations in **85** can be exchanged with cationic dyes due to the anionic framework. The results of the paper suggest that the dye molecules in dye@**85** can be gradually released in the presence of NaCl. Therefore, releasing the dyes were an ion-exchange process in this study.[118]

3.2.4 Luminescence properties. The IFMC-2 (**85**) MOF that was introduced beforehand can be also utilized as a potential luminescent probe towards different Ln^{3+} ions. As we mentioned beforehand, the anionic framework of **85** allowed cation-exchange experiments to be performed, in which the $[HDMA]^+$ ions could be exchanged with Ln^{3+} cations. In this sense, the group tried to load Ln^{3+} ions into the cavities of **85** and then analyzed the luminescent properties of the resulting material. The emission spectra of the as-prepared Ln^{3+}-loaded MOFs indicated that **85** was suitable for the sensitization of Tb^{3+} and Dy^{3+} ions rather than Eu^{3+} and Sm^{3+} emitters.[118]

The 3D lanthanide anionic MOF $\{K_5[Ln_5(IDC)_4(ox)_4]\}_n\cdot(20H_2O)_n$, (Ln = Gd (**86**), Tb (**87**), and Dy (**88**)) show luminescent properties that are induced by cation-exchange. The luminescent studies revealed that the luminescent properties of **86–88** can be changed through the exchange of the guest K^+ ions with various cations. To examine the possibility of modifying the luminescent properties through cation-exchange, a solid sample of **87** was soaked in DMF containing various metal cations. The luminescent intensity in the presence of 3 equiv. of Ca^{2+} ions was about twice as strong as that found without Ca^{2+} ions. However, the luminescent intensities did not change or increase in the presence of 3 equiv. of Na^+, NH_4^+, Mg^{2+}, Sr^{2+}, Ba^{2+}, Zn^{2+}, Cd^{2+}, Hg^{2+} and Pb^{2+} cations. When 1–3 equiv. of transition-metal ions, such as Mn^{2+}, Fe^{2+}, Co^{2+}, Ni^{2+} and Cu^{2+}, were added to the emulsion of **87** in DMF, the luminescent intensity was not enhanced but rather weakened dramatically or even quenched. As a result, they noted that compound **87** was the first lanthanide-based MOF to be used as a promising Ca^{2+} ion-selective luminescent probe and it can also show a remarkable increase in the luminescent emission of Tb(III) upon the addition of Ca^{2+} ions, while the exchange of K^+ ions with other cations did not modulate the luminescence emission of this compound.[119]

Another polymer that shows a cation-exchange role in the luminescent sensing of aqueous metal ions is $[NH_4]_2[ZnL']\cdot 6H_2O$ (**89**), which has been studied by Sh. Liu and co-workers. Polymer **89** was soaked in aqueous solutions of MCl_x {M = Na^+, K^+, Mg^{2+}, Ca^{2+}, Mn^{2+}, Ni^{2+}, Co^{2+} and Cu^{2+}} to form a metal-ion infused phase (M@**89**). The research group indicated that the luminescence intensity of M@**89** was highly dependent on the nature of the doped metal ion. For polymer **89**, there are two types of suitable counter ions for cation-exchange: (i) Zn(II) ions and (ii) $[NH_4]^+$ ions. Their suggestion shows that in the Cu@**89** sample, cation-exchange occurs between (NH_4^+) and Cu(II), rather than between Zn(II) and Cu(II). In this study, the cation-exchange materials also performed as potential luminescent sensors of aqueous metal ions.[120]

The last example in this section is MOF_COOH, $[Zn_3$(-Httca)$_2$(4,4′-bpy)$(H_2O)_2]_n$ (**90**), which was prepared by J. Cao *et al.* The uncoordinated carbonyl groups in the channels of **90** can act as post-synthetic modification sites for cation-exchange. During the exchange, Na^+ cations were loaded into the pores of **90**. As a matter of fact, they reported that the MOFs have several advantages that make them useful for sensitizing lanthanide cations. Thus, they also loaded lanthanide cations into the pores *via* a post-synthetic cation-exchange (Ln = Sm^{3+}, Eu^{3+}, Dy^{3+} or Tb^{3+}). In addition, photoluminescence studies were performed on each sample of **81**, Na^+@**81** and Ln^{3+}@**90**. It is significant in their study that the Ln^{3+}-loaded **90** sample exhibited very interesting photoluminescence properties. These materials showed a very similar emission to Na^+@MOF-COO^-,

but with different intensity. The results of their experiments indicated that the microporous metal–organic open framework, reported in the paper, was not suitable for the sensitization of Sm^{3+}, Dy^{3+} and Eu^{3+} emitters.[121]

3.2.5 Detection of ions. Another ability that can be achieved using the exchanged samples of MOFs is being a selective and sensitive luminescence sensor probe for the detection of ions. A new series of Ln-MOFs was prepared with this aim. LnL″ (**91**) (Ln = La (**92**), Y (**93**), Eu (**94**), Tb (**95**) and Gd (**96**)) were prepared under hydrothermal conditions. The compounds exhibit layer-like structures with the $[HDMA]^+$ cations located in their channels. The cations in the channels can be easily replaced by a number of metal ions. After cation-exchange experiments with a series of metal ions, **94** exhibited an efficient quenching phenomenon upon the typical Eu-luminescence in the case of Fe^{3+} ions. They also presented the luminescent material, **94**, as a highly selective fluorescent probe aimed for Fe^{3+} ions, and the possible sensing mechanism was further explored.[122]

One more MOF has been reported with this ability. Zh. Chen *et al.* reported $[HDMA][Eu(H_2O)_2(BTMIPA)]\cdot 2H_2O$ (**97**) and studied the cation-exchange between $[HDMA]^+$ and metal ions. In this study, Fe^{3+} and Al^{3+} were initially exchanged with the $[HDMA]^+$ cations in the channels and the framework of **97** may have been faced with the exchange between Fe^{3+}/Al^{3+} and Eu^{3+}.

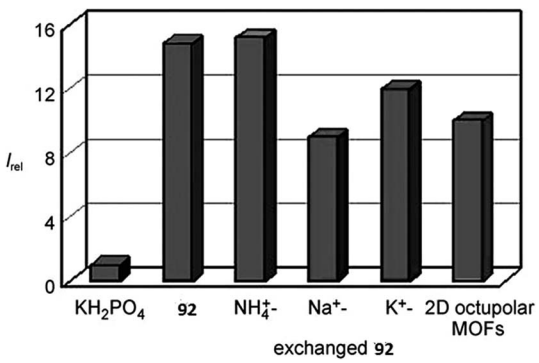

Fig. 16 A comparison of the SHG-intensities of different materials. Reproduced with permission from ref. 124, copyright 2007, John Wiley & Sons.

A decrease in the photoluminescence intensity of the Al^{3+}-loaded sample was observed. Therefore, the cation-exchange resulted in a complex that can selectively sense Fe^{3+} and Al^{3+} ions through fluorescence quenching and enhancement. To further prove that the fluorescence quenching and enhancement were caused by a cation-exchange process, detailed studies on the luminescence properties of **97** in the presence of Fe^{3+} and Al^{3+} were carried out. With increasing time, the photoluminescence intensity decreased for the Fe^{3+}-loaded sample, but increased for the Al^{3+}-loaded sample. This result indicates that, according to the replacement of cations in channels with Fe^{3+} and Al^{3+}, they had a notable effect on the fluorescence emissions.[123]

3.2.6 Other applications. The effect of different cations during the cation-exchange experiment on SHG intensities has been discussed. The synthesis of $[(HDMA)_2Cd_3(C_2O_4)_4]\cdot MeOH\cdot 2H_2O$ (**98**) has been reported as an example. This open framework showed high ion-exchange capacities between $[HDMA]^+$ and the cations NH_4^+, Na^+ and K^+. Then, all of the exchanged samples were studied to check the effect of the cation on the SHG response (Fig. 16). To examine the result of a low crystallinity on the SHG intensity of the host framework by cation-exchange, the group replaced Na^+ ions in the exchanged sample (low crystallinity) by the $[HDMA]^+$ species again. The re-exchanged product was also found to show low crystallinity, but displayed a powder SHG intensity. Therefore, the decrease in the crystallinity of the host framework had no apparent effect on its SHG behavior and the change of the SHG intensity on cation-exchange may be a cation-dependent phenomenon.[124]

The last application of ion-exchange processes that has been noticed in our study is in two-photon-pumped dye lasers, which are very important because of their various applications. J. Yu and co-workers connected them to cation encapsulation in an anionic MOF. Generally, they demonstrated a new two-photon-pumped micro-laser by encapsulating a cationic pyridinium hemicyanine dye into an anionic MOF. Thus, Bio-MOF-1 ($Zn_8(Ad)_4(BPDC)_6O\cdot 2HDMA$) (**99**) was synthesized, in which the $HDMA^+$ cations were located in the channels that allowed the introduction of the cationic dye DMASM *via* an ion-exchange process. On the other hand, most of the $HDMA^+$ cations in the as-synthesized **99** were replaced by the DMASM cations in **99** × DMASM (Fig. 17). The enhanced fluorescence of

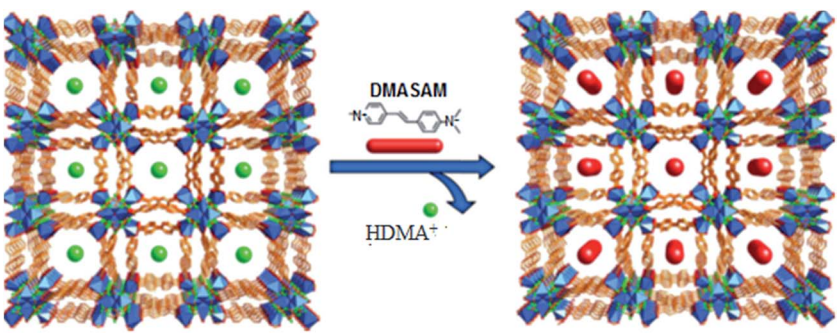

Fig. 17 Encapsulation of DMASM dye into ($Zn_8(Ad)_4(BPDC)_6O\cdot 2HDMA$) (**99**). Reproduced with permission from ref. 125, copyright 2013, Nature publish group.

Table 2 A summary of ionic nanoporous metal–organic frameworks, the post-synthetic ion-exchange process in them and their resulting properties and applications

MOFs formula	Type of exchange	Type of exchanged species	The resulting properties or applications	Ref.
$[Ni_2(C_{28}H_{52}N_{10})]_3[BTC]\cdot 6C_5H_5N\cdot 36H_2O$ (**1**)	Anionic	I_3^- anions in the channels	—	49
$[\{Cd(H_2O)_3\}_{34}(N_4C_6H_{12})_{17}]Cl_{68}\cdot 46H_2O\cdot 68DMF$ (**2**)	Anionic	SCN^- by Cl^-	—	50
$[Co(4\text{-pyrdpm})_3AgBF_4]$ (**3**)	Anionic	—	—	52
$[Co(4\text{-pyrdmp})_3AgOTf]$; (4-pyrdpm) (**4**)	Anionic	PF_6^- by triflate	—	52
$[Ni(timpt)_2](ClO_4)_2$ (**5**)	Anionic	ClO_4^- by NO_3^-/ClO_4^- by $NaBF_4^-$	—	53
$\{[Ag_3(1,3,5\text{-Tris})_2X_2]X\}_n$ (X = ClO_4^- (**6**))	Anionic	ClO_4^- by NO_3^-	—	54
$\{[Ag_3(1,3,5\text{-Tris})_2X_2]X\}_n$ (X = NO_3^- (**7**))	Anionic	NO_3^- by ClO_4^-	—	54
$\{[Cu(2\text{-}(2\text{-Pyridyl}))_2](ClO_4)(H_2O)_{1/2}\}_n$ (**8**)	Anionic	ClO_4^- by $C_6H_5COO^-$	—	55
$(NBU_4)_m(A)_n\{Zn(mim)_2\}_6$ (**9**)	Anionic	OH^- by HCO_3^- or CO_3^{2-}	—	56
$[M(\beta\text{-Diketone})_3Ag_3]\text{-}X_2\cdot$solv (**10**) $[ZnL_3Ag_3]X_2\cdot$solv as host network {X = BF_4^-, ClO_4^-, $CF_3SO_3^-$, PF_6^-}	Anionic	BF_4^-, ClO_4^-, $CF_3SO_3^-$, PF_6^- by each other	—	57
$[M_3X_2]\cdot[HDMA]_2\cdot 8DMA$ (M = Co (**11**))	Cationic	$HDMA^+$ by Na^+	—	63
$[M_3X_2]\cdot[HDMA]_2\cdot 8DMA$ (M = Mn (**12**))	Cationic	$HDMA^+$ by Na^+	—	63
$(HDMA)_3[In_3(BTB)_4]\cdot 12DMF\cdot 22H_2O$ (ZJU-28) (**13**)	Cationic	$Me_2NH_2^+$ by Cu^{2+}, Ni^{2+} and Eu^{3+}	—	64
$[HDMA][In(mdip)]\cdot 2.5DMF\cdot 4H_2O$ (**14**)	Cationic	$HDMA^+$ by (M = Li^+, Na^+, K^+, Mg^{2+}, Ca^{2+}, Sr^{2+}, Ba^{2+}, Cu^{2+}, Fe^{3+})	—	65
$[HDMA][M_2(bptc)(\mu_3\text{-}OH)(H_2O)_2]$ (**15**)	Cationic	$[HDMA]^+$ by Li^+, Na^+ and K^+	—	66
$H_2Na_4[Cu_{12}(OH)_6\text{-}(PZ)_6(BTC)_6]\cdot 23H_2O$ (**16**)	Cationic	Na^+ by Li^+, K^+ and Cs^+/Cu^{2+}, Ni^{2+} and Mn^{2+}	—	67
$[Ga_6(1,3,5\text{-BTC})_8\cdot 6DMA\cdot 3DMF\cdot 26H_2O]$ (Ga·MOF-1) (**17**)	Cationic	Ga^+ by Li^+ and Na^+	—	69
$[In_{48}(C_5N_2O_4H_2)_{96}(C_2N_3H_{15})_{24}(DMF)_{36}\text{-}(H_2O)_{192}]$ (**18**)	Cationic	The cationic guest molecules by other cations	—	70
$[Na_{48}^+(H_2O)_{282}][In_{48}(C_5N_2O_4H_2)_{96}]$ (**19**)	Cationic	—	—	70
$In_{48}(C_5H_2N_2O_4)_{96}(C_7N_3H_{15})_{24}(C_3H_7NO)_{36}(H_2O)_{192}$ (**20**)	Cationic	Organic cations by Na^+/acridine orange (AO)	—	71
$[In_3O(pba)_3(ndc)_{1.5}](NO_3)$ (**21**)	Anionic	—	Separation process {for use as drug carriers}	72
$[In_3O(pba)_3(bpdc)_{1.5}](NO_3)$ (**22**)	Anionic	NO_3^- by OG^{2-}	Separation process {for use as drug carriers}	72
$[CuL_2(H_2O)_{0.5}](NO_3)_2$ (**23**)	Anionic	NO_3^- by Cl^-, Br^-, I^-, SCN^- and N_3^-	Could be an anion separator to separate these anions	73
$ZnCl_2(BPu)$ (**24**)	Anionic	Cl^- by ClO_4^-, NO_3^- and SO_4^{2-}	Separation of anions from water	74
$ZnI_2(BPu)$ (**25**)	Anionic	I^- by ClO_4^-, NO_3^- and SO_4^{2-}	Separation of anions from water	74
$ZnBr_2(BPu)$ (**26**)	Anionic	Br^- by ClO_4^-, NO_3^- and SO_4^{2-}	Separation of anions from water	74
$\{[Dy_2Zn(BPDC)_3(H_2O)_4](ClO_4)_2\cdot 10H_2O\}_n$ (**27**)	Anionic	ClO_4^- by CrO_4^{2-}	Separation of pollutant anions from water; considered as a luminescent probe	78
$Ag_2(4,4'\text{-bipy})_2(O_3SCH_2CH_2SO_3)\cdot 4H_2O$ (**28**)	Anionic	EDS^- by MnO_4^-, ReO_4^-, and CrO_4^{2-}	Separation of pollutant anions from water	80
$[Zn_2(Tipa)_2(OH)]\cdot 3NO_3\cdot 12H_2O$ (**29**)	Anionic	NO_3^- by $Cr_2O_7^{2-}$	Separation of pollutant anions from water	81
$[Zn(Tipa)]\cdot 2NO_3\cdot DMF\cdot 4H_2O$ (**30**)	Anionic	NO_3^- by $Cr_2O_7^{2-}$	Separation of pollutant anions from water	81
$[Ag_2(btr)_2]2ClO_4\cdot 3H_2O$ (**31**)	Anionic	ClO_4^- by $Cr_2O_7^{2-}$	Separation of pollutant anions from water – considered as a luminescent probe	82

Table 2 (*Contd.*)

MOFs formula	Type of exchange	Type of exchanged species	The resulting properties or applications	Ref.
ZJU-101 (**32**)	Anionic	NO_3^- by $Cr_2O_7^{2-}$	Separation of pollutant anions from water	86
$[\{Ni_2(Lig)_3\text{-}(SO_4)(H_2O)_3\}\cdot(SO_4)\cdot x(G)]_n$ (**33**)	Anionic	SO_4^{2-} by $Cr_2O_7^{2-}$ and MnO_4^-	Separation of pollutant anions from water	87
$[Cu(II)(bped)_2(H_2O)_2(SiF_6)]I\cdot 4H_2O$ (Cu-MOF-SiF_6) (**34**)	Anionic	SiF_6^{2-} by NO_3^-	Catalytic activity in the selective oxidation of benzylic compounds/MeOH adsorption, desorption/EtOH adsorption, desorption	89
$[Cu(II)(bped)_2(H_2O)_2(NO_3)]I\cdot 4H_2O$ (Cu-MOF-NO_3)h (**35**)	Anionic	—	Catalytic activity in the selective oxidation of benzylic compounds/MeOH adsorption, desorption/EtOH adsorption, desorption	89
$Ag_2(4,4'\text{-bipy})_2(O_3SCH_2CH_2SO_3)\cdot 4H_2O$ (**28**)	Anionic	Organosulfonate by various inorganic species	Catalytically active in heterogeneous ketal formation	91
$Cu_2(4,4'\text{-bipy})_2(O_3SCH_2CH_2SO_3)\cdot 3H_2O$ (**36**)	Anionic	Organosulfonate by various inorganic species	Catalytically active in heterogeneous ketal formation	91
$[Ln(TTP)_2]\cdot(CF_3SO_3)_3\cdot C_3H_6O\cdot 5H_2O$ (Ln = Eu (**37**))	Anionic	CF_3^- by ClO_4^- and SCN^-	Luminescent properties	92
$[Ln(TTP)_2]\cdot(CF_3SO_3)_3\cdot C_3H_6O\cdot 5H_2O$ (Ln = Gd (**38**)	Anionic	CF_3^- by ClO_4^- and SCN^-	—	92
$[\{Zn(L)(MeOH)_2\}\text{-}(NO_3)_2\cdot xG]_n$ (**39**)	Anionic	NO_3^- by ClO_4^- and $N(CN)_2^-$ (type A) and N_3^- and SCN^- (type B)	Having tunable luminescent behavior	93
[Ln(bipyNO$_4$)][Tfo)$_3\cdot$x$\cdot$solvent (Ln = Tb, Dy, Ho, Er) (**40**)	Anionic	$[Tfo]^-$ by POM^-	Preserving slow magnetic relaxation	95
$[Cd(4\text{-Amino})_2(ClO_4)_2]\cdot H_2O$ (**41**)	Anionic	ClO_4^- by the I_3^-	Used for the detection of the enrichment of IO_3^- in dilute solutions	96
$NH_4[Cu_3\text{-}(\mu_3\text{-}OH)(\mu_3\text{-}4\text{-cpy})_3]$ (NH_4@1) (**42**)	Cationic	NH_4^+ by Li^+, Na^+, K^+, $Ca^{2+}/2$, $La^{3+}/3$, Et_3NH^+ and Me_3NH^+	N_2 adsorption/separation selectivity by the adsorption of gases such as N_2, CH_4, CO_2, C_2H_2 and harmful vapors (benzene, cyclohexane)	97
$[HDMA]_3[(Cu_4Cl)_3\text{-}(btc)_8]\cdot 9DMA$ (**43**)	Cationic	$HDMA^+$ by organic cations	Gas separation (CO_2/N_2)/N_2, CO_2 or H_2 adsorption	98
$[HDMA]_3[(Cu_4Cl)_3\text{-}(btc)_8]\cdot 9TMA$ (**44**)	Cationic	$HDMA^+$ by organic cations	Gas separation (CO_2/N_2))/N_2, CO_2 or H_2 adsorption	98
$[HDMA]_3[(Cu_4Cl)_3\text{-}(btc)_8]\cdot 9TEA$ (**45**)	Cationic	$HDMA^+$ by organic cations	Gas separation (CO_2/N_2))/N_2, CO_2 or H_2 adsorption	98
$[HDMA]_3[(Cu_4Cl)_3\text{-}(btc)_8]\cdot 9TPA$ (**46**)	Cationic	$HDMA^+$ by organic cations	Gas separation (CO_2/N_2))/N_2, CO_2 or H_2 adsorption	98
$[Zn_{17}thb_{14}(\mu_4\text{-}O)_4(H_2O)(HDMA)]\cdot Me_2NH_2\cdot$xguest (**47**)	Cationic	Zn^{2+} by Pd^{2+} and Ag^+	—	99
$[Pd_{17}thb_{14}(\mu_4\text{-}O)_4(H_2O)(HDMA)]\cdot Me_2NH_2\cdot$xguest (**48**)	Cationic	$Me_2NH_2^+$ by Pd^+ or Ag^+	Catalytic properties	99
$[Ag_{17}thb_{14}(\mu_4\text{-}O)_4(H_2O)(HDMA)]\cdot Me_2NH_2\cdot$xguest (**49**)	Cationic	$Me_2NH_2^+$ by Pd^+ or Ag^+	Catalytic properties	99
$(HDMA)_3[In_3(BTB)_4]\cdot 12DMF\cdot 22H_2O$ (ZJU_28) (**50**)	Cationic	$HDMA^+$ by cationic transition metal complexes	Used as a recyclable catalyst for alkene hydrogenation	100

Table 2 (*Contd.*)

MOFs formula	Type of exchange	Type of exchanged species	The resulting properties or applications	Ref.
$[HDMA]_2[Zn_2(BDC)_3(DMA)_2]\cdot 6DMF$ (**51**)	Cationic	$[HDMA^+]$ by Ni^{2+} (**53**), Na^+ (**54**), Li^+ (**55**), (TEA^+) (**56**) and $(TPA)^+$ (**57**)	Catalytic activity	101 and 102
$\|(HPP^{2+})_{24}\|[In_{48}(HImDC)_{96}]$ (HPP-*rho*-ZMOF) (**57**)	Cationic	(HPP^{2+}) by $HDMA^+$, Li^+ (**59**), Mg^{2+}	H_2 adsorption	103
Rho_ZMOF (**59**)	Cationic	By Li^+, Na^+, K^+ and Cs^+	H_2 adsorption	104
Sod_ZMOF (**60**)	Cationic	By Li^+, Na^+, K^+ and Cs^+	H_2 adsorption	104
$\{[Hdma](H_3O)][In_2(L)_2]\cdot 4DMF\cdot 5H_2O\}_\infty$ (**61**)	Cationic	Organic cation by Li^+	N_2 adsorption	105
$\{[(H_2ppz][In_2(L)_2]\cdot 3.5DMF\cdot 5H_2O\}_\infty$ (**62**)	Cationic	Organic cation by Li^+	N_2 adsorption	105
$\{[(H_2ppz][In_2(L)_2]\cdot 4DMF\cdot 5.5H_2O\}_\infty$ (**63**)	Cationic	Organic cation by Li^+	H_2 adsorption/H_2 storage/N_2 adsorption	105
$\{Li_{1.4}(H_3O)_{0.6}][In_2(L)_2]\cdot 4\text{-acetone}\cdot 11H_2O\}_\infty$ (**64**)	Cationic	—	H_2 adsorption/H_2 storage/N_2 adsorption	105
$\{[(H_2ppz][In_2(L)_2]\cdot 3.5DMF\cdot 5H_2O\}_\infty$ (**65**)	Cationic	H_2PPZ^{2+} by Li^+	H_2 and N_2 adsorption	106
$\{[Li_{1.5}(H_3O)_{0.5}][In_2(L)_2]\cdot 4\text{-acetone}\cdot 11H_2O\}_\infty$ (**66**)	Cationic	—	H_2 adsorption	106
Do-MOF (**67**)	Cationic	Hydroxyl protons by Li^+ and Mg^{2+}	H_2 adsorption	107
$([In_{80}(Himdc)_{160}]^{80-})_n$ (Usf-ZMOF) (**68**)	Cationic	$[1,2\text{-}H_2dach]^+$ by Li^+, Na^+ and Mg^{2+}	H_2 adsorption	108
$\{(A)[In(L^n)]\cdot solv\}_\infty$, (A = $1/2H_2PPZ^{2+}$ or $HDMA^+$, solv = DMF, CH_3CN and H_2O) (**69**)	Cationic	H_2PPZ^{2+} or $Me_2NH_2^+$ by Li^+	H_2 and N_2 adsorption	109
$Zn_8(ad)_4(BPDC)_6 0.2HDMA$ (**70**)	Cationic	$HDMA^+$ by TMA^+, TEA^+ and TBA^+	CO_2 adsorption	110
Sod-ZMOFs (**71**)	Cationic	By alkali-metals such as: Li^+, Na^+, K^+ (**73**) and Cs^+	CO_2 adsorption	111
4,6_PmDc $[In\text{-}(C_6N_2O_4H_2)_2Na_{0.36}K_{1.28}](NO_3)_{0.64}(H_2O)_{2.1}$ (**73**)	Cationic	K^+ by Li^+	N_2 and Ar adsorption	112
$\{(HDMA)_2[Zn_3(BDC)_4]\cdot DMF\cdot H_2O\}$ (**74**)	Cationic	$HDMA^+$ by Cu^{2+} (**76**), Li^+ (**77**) and Na^+ (**78**)	N_2 adsorption	114
$[(CH_3)_3NH][NaVO(BTC)_{4/3}]\cdot 0.5DMF$ (**78**)	Cationic	The organic amine cations by transition metal ions	N_2 adsorption	115
$\{[(CH_3)_4N]_3LiVO(BTC)_2\}$ (**79**)	Cationic	The organic amine cations by transition metal ions	N_2 adsorption	115
$[Zn_2(BDC)_3(DMA)_2]\cdot 6DMF$ (**51**)	Cationic	$HDMA^+$ by Ni^{2+} (**53**), Na^+ (**54**), Li^+ (**55**), Cu^{2+} (**81**) and K^+ (**82**)	CH_4 adsorption	116
$(C_4H_{12}N)_2[Cu_{12}(BTC)_8\cdot 12H_2O][HPW_{12}O_{40}]\cdot 25H_2O$ (**82**)	Cationic	$(CH_3)_4N^+$ by K^+ and Li^+	VOCs adsorption/N_2 adsorption	117
$K_2[Cu_{12}(BTC)_8\cdot 12H_2O][HPW_{12}O_{40}]\cdot 28H_2O$ (**83**)	Cationic	—	VOCs adsorption/N_2 adsorption	117
$Li_2[Cu_{12}(BTC)_8\cdot 12H_2O][HPW_{12}O_{40}]\cdot 28H_2O$ (**84**)	Cationic	—	VOCs adsorption/N_2 adsorption	117
$[HDMA]_4[(Zn_4dttz_6)Zn_3]\cdot 15DMF\cdot 4.5H_2O$ (**85**)	Cationic	$[HDMA]^+$ by Ln^{3+}	The adsorption of cationic dyes/ luminescent properties: suitable for the sensitization of Tb^{3+} and Dy^{3+} ions rather than Eu^{3+} and Sm^{3+} emitters	118
$\{K_5[Ln_5(IDC)_4(ox)_4]\}_n\cdot(20H_2O)_n$, (Ln = Gd (**86**))	Cationic	K^+ ions with various cations	Luminescent properties	119
$\{K_5[Ln_5(IDC)_4(ox)_4]\}_n\cdot(20H_2O)_n$, (Tb (**87**))	Cationic	K^+ ions with various cations	Luminescent properties	119
$\{K_5[Ln_5(IDC)_4(ox)_4]\}_n\cdot(20H_2O)_n$, (Dy (**88**))	Cationic	K^+ ions with various cations	Luminescent properties	119
$[NH_4]_2[ZnL']\cdot 6H_2O$ (**89**)	Cationic	$[NH_4]^+$ by Na^+, K^+, Mg^{2+}, Ca^{2+}, Mn^{2+}, Ni^{2+}, Co^{2+} and Cu^{2+}	The luminescent sensing of aqueous metal ions	120
$[Zn_3(Httca)_2(4,4'\text{-bpy})(H_2O)_2]_n$ (**90**)	Cationic	The uncoordinated carbonyl groups located in the channels by Na^+ and (Ln = Sm^{3+}, Eu^{3+}, Dy^{3+} or Tb^{3+})	Photoluminescence properties	121
LnL″ (**91**) (Ln = La (**92**), Y (**93**), Eu (**94**), Tb (**95**) and Gd (**96**)) {L″ = tetrakis[4-(carboxyphenyl)oxamethyl] methane}	Cationic	$[HDMA]^+$ by a number of metal ions	The detection of ions	122

Table 2 (*Contd.*)

MOFs formula	Type of exchange	Type of exchanged species	The resulting properties or applications	Ref.
$[HDMA][Eu(H_2O)_2(BTMIPA)]\cdot 2H_2O$ (**97**)	Cationic	Firstly, $[HDMA]^+$ by Fe^{3+} and Al^{3+}, secondly Fe^{3+}/Al^{3+} by Eu^{3+}	The detection of ions	123
$[(HDMA)_2Cd_3(C_2O_4)_4]\cdot MeOH\cdot 2H_2O$ (**98**)	Cationic	$[HDMA]^+$ by NH_4^+, Na^+ and K^+	Effect SHG intensities	124
$(Zn_8(Ad)_4(BPDC)_6O\cdot 2HDMA)$ (**99**)	Cationic	$HDMA^+$ by DMASM cations	Enhanced fluorescence	125

99 × DMASM was also observed. Such a notable emission enhancement showed the pore confinement of DMASM molecules within **99**.[125] A summary of all the points discussed about MOF ion-exchange are shown in Table 2.

4. Conclusion

Metal organic frameworks (MOFs) constitute an important field of study due to their ease of synthesis and high surface areas in certain cases. Moreover, a wide range of MOFs can be employed to exhibit various abilities, which are because of their construction. MOFs include a framework with different materials in their channels. These frameworks can be anionic, cationic or neutral. In some cases, various ions fill the channels, which can be exchanged with other organic or inorganic ions. Therefore, the synthesis, characterization and ion-exchange properties of MOFs have become important fields of study. Thus, for improvement in this field of study, it is necessary to reach a better understanding of these materials and their ion-exchange mechanisms. In this study, we have summarized most of the reports on ion-exchange experiments that occur in the pores of MOFs reported to date. There are two types of ion-exchanges (cation-exchange and anion-exchange) that we have discussed separately. Active cations have been successfully introduced into a series of anionic MOFs *via* cation-exchange reactions. Zeolite-like MOFs (ZMOFs) also have an anionic framework and remain in this group. ZMOFs include two topologies that have been named Rho and Sod. Most of the cation-exchange processes are observed in the Rho-topology. We also conclude that metal ions with higher charge and coordination numbers are more susceptible to construct cationic metal–ligands framework. The selectivity of this exchange depends mainly on the size of the pore openings, the electrostatic interactions between the anionic framework and the cationic guest and finally the concentration of the ions in solution. In addition, cationic frameworks exhibit anion-exchange in their pores too. One important observation is that several experiments described represent a certain single-crystal-to-single-crystal transformation. Another important observation is that most of the experiments indicate anion-exchange against the generally reported trends for anion coordinative ability. Discussing the important applications that appear after the exchange process is another important part of this study. For both, cation- and anion-exchange, we classified these applications to five groups: separation processes, catalytic properties, adsorption, luminescence properties and others. In regard to anion-exchange, we noticed that MOFs have also been studied for the removal of hazardous organic materials from water. These compounds have attracted a considerable amount of attention due to their high surface area, uniform pore size, controllable structures, and tailorable functions. These cationic coordination compounds can serve as promising anion exchange materials through the selective exchange of charge balancing anions in the framework with other anions, leading to tunable changes in their physical properties. The charge-balancing anions usually occupy the framework voids and are sometimes just weakly coordinated or even uncoordinated to

the metal centers, potentially allowing the capture and separation of anions through anion exchange. Because of these reasons, there are some examples of separating different anions from water that we collected in our study. Moreover, comparing cation-exchange with anion-exchange, we have shown that the adsorption of different gases with only the anionic framework has been observed and this was due to their cation-exchange experiments. In this context, H_2 and N_2 were used for further experiments. In the subject of H_2 adsorption, the efficient frameworks that have been utilized several times were Rho-ZMOFs, whereas, the Sod-topology of ZMOFs were only used for CO_2 adsorption. A wide range of gas adsorption was observed in the case of the exchanged materials bearing Li^+ cations. The subject of CH_4 adsorption has a few reports published to date and it has ambient reportage. Working on more applications, particularly the gas adsorption of the exchanged-materials of MOFs, can be worth aspiring to. It seems that post-synthetic ion-exchange and the cation-exchange process are suitable methods for modulating the properties of metal organic frameworks.

Abbreviations

CPs	Coordination polymers
(BOF-1,1)	$[Ni_2(C_{28}H_{52}N_{10})]_3[BTC]\cdot 6C_5H_5N\cdot 36H_2O$
Bismacrocyclic nickel(II)	$[Ni_2(C_{26}H_{52}N_{10})\text{-}(Cl)_4]\cdot H_2O$
BTC	1,3,5-Benzenetricarboxylate
DMF	*N*,*N*-Dimethyl formamide
(MOF-Co/$AgBF_4$-1)	$[Co(4\text{-pyrdpm})_3AgBF_4]$
(MOF-Co/AgOTf-1)	$[Co(4\text{-pyrdmp})_3AgOTf]$
(4-pyrdpm)	5-(4-Pyridyl)-4,6-dipyrrinato
timpt	2,4,6-Tris[4-(imidazole-1-ylmethyl)phenyl]-1,3,5-triazine
1,3,5-tris	1,3,5-Tris(pyrazol-1-yl)benzene
2-(2-pyridyl)	2-(2-Pyridyl)-5-(4-pyridyl)-1,3,4-oxadiazole
ZIF	Zeolitic imidazolate framework
β-diketone	1,3-Bis(4′-cyanophenyl)-1,3-propanedionato
H_4X	Tetrapodal ligand tetrakis[4-(carboxy phenyl) oxamethyl]methan acid
H_3BTB	4,4′,4″-Benzene-1,3,5-triyl-tribenzoic acid
H_4mdip	5,5′-Methylenediisophtalic acid
H_4bptc	3,3′,4,4′-Biphenyltetracarboxylic acid
PZ	Pyrazolate
HPP	1,3,4,6,7,8-Hexahydro-2*H*-pyrimido[1,2-*a*] pyrimidine
ina	Isonicotinate
pba	4-(Pyridine-4-yl)benzoate
bdc	Terephthalate
NH_2-bdc	2-Aminoterephthalate
ndc	2,6-Naphthalenedicarboxylate
bpdc	4,4′-Biphenyldicarboxylate
ITC-3	$[In_3O(pba)_3(ndc)_{1.5}](NO_3)$
ITC-4	$[In_3O(pba)_3(bpdc)_{1.5}](NO_3)$
BPu	*N*,*N*′-Bis(*m*-pyridyl)urea
DMA	Dimethylamine
BPDC	4,4′-Dicarboxylate-2,2′-dipyridine anion
LDH	Layered double hydroxide
EDS	1,2-Ethanedisulfonate
Tipa	Tris(4-(1*H*-imidazol-1-yl)phenyl)amine
btr	4,4′-Bis(1,2,4-triazole)
H_2bpydc	2,2′-Bipyridine-5,5′-dicarboxylate
Lig	Tris(4-(1*H*-imidazol-1-yl)phenyl)amine
bped	*meso*-1,2-Bis(4-pyridyl)-1,2-ethandiol
SLUG-22	$Cu_2(4,4'\text{-bipy})_2(O_3SCH_2CH_2SO_3)\cdot 3H_2O$
TfO	Triflate
bipyNO	4,4′-Bypyridyl-*N*,*N*′-dioxide
POM	Polyoxometalates
4-amino	4-Amino-3,5-bis(4-pyridyl-3-phenyl)-1,2,4-triazole
4-cpy	Carboxypyrazolato
DMA	*N*,*N*-Dimethylamide
TMA	Tetramethylammonium
TEA	Tetraethylammonium
TPA	Tetrapropylammonium
HImDC	Imidazoledicarboxylate
H_3ImDC	4,5-Imidazoledicarboxylic acid
H_2thb	2,5-Thiophenedicarboxylate
NOTT-206-solv	$\{[(Hdma)(H_3O)][In_2(L)_2]\cdot 4DMF\cdot 5H_2O\}_\infty$
NOTT-200-SOLV	$\{[(H_2ppz)][In_2(L)_2]\cdot 3.5DMF\cdot 5H_2O\}_\infty$
NOT-208-solv	$\{[(H_2ppz)][In_2(L)_2]\cdot 4DMF\cdot 5.5H_2O\}_\infty$
ppz	Piperazine
NOT-209-solv	$\{Li_{1.4}(H_3O)_{0.6}[In_2(L)_2]\cdot 4\text{-acetone}\cdot 11H_2O\}_\infty$
H_4L	Tetracarboxylate isophthalic acid
1-ppz-solv	$\{[(H_2ppz)][In_2(L)_2]\cdot 3.5DMF\cdot 5H_2O\}_\infty$
1-Li-solv	$\{[Li_{1.5}(H_3O)_{0.5}][In_2(L)_2]\cdot 4\text{-acetone}\cdot 11H_2O\}_\infty$
Himdc	4,5-Imidazoledicarboxylate
1,2-dach	1,2-Diaminocyclohexane
TBA	Tetrabutylammonium
ad	Adeninate
BPDC	Biphenyl dicarboxylate
4,6-PmDc	4,6-Pyrimidicarboxylate
$HMDA^+$	Dimethylamonnium
NENU-3	$(C_4H_{12}N)_2[Cu_{12}(BTC)_8\cdot 12H_2O][HPW_{12}O_{40}]\cdot 25H_2O$
NENU-28	$K_2[Cu_{12}(BTC)_8\cdot 12H_2O][HPW_{12}O_{40}]\cdot 28H_2O$
BDC^{2-}	1,4-Benzenedicarboxylate
H_3dttz	4,5-Di(1*H*-tetrazol-5-yl)-2*H*-1,2,3-triazole
IDC^{3-}	Imidazole-4,5-dicarboxylate
L′	1,2,4,5-Benzenetetracarboxylate
H_4ttca	1,1′:2′,1″-Terphenyl-4,4′,4″,5′-tetracarboxylic acid
L″	Tetrakis[4-(carboxyphenyl)oxamethyl] methane
SHG	Second harmonic generation
BPDC	Biphenyldicarboxylate
DMASM	4-[*p*-(Dimethylamino)styryl]-1-methylpyridinium
$H_4BTMIPA$	5,5′-Methylenebis(2,4,6-trimethyl sophtalic acid)
LDH	Layered double hydroxide

Acknowledgements

The authors would like to acknowledge the financial support of University of Tehran for this research under grant number 01/1/389845.

References

1 K. Akhbari and A. Morsali, *Coord. Chem. Rev.*, 2010, **257**, 1972–1981.
2 S. Hojaghani, K. Akhbari, M. H. Sadr and A. Morsali, *Inorg. Chem. Commun.*, 2014, **44**, 1–5.
3 S. Kitagawa and K. Uemura, *Chem. Soc. Rev.*, 2005, **34**, 109–119.
4 K. Akhbari, S. Beheshti, A. Morsali, V. Yilmaz and O. Büyükgüngör, *J. Mol. Struct.*, 2014, **1074**, 279–283.
5 T. Uemura and S. Kitagawa, *Chem. Lett.*, 2005, **34**, 132–137.
6 K. Akhbari, A. Morsali and P. Retailleau, *Ultrason. Sonochem.*, 2013, **20**, 1428–1435.
7 S. Wu, X. Shen, B. Cao, L. Lin, K. Shen and W. Liu, *J. Mater. Sci.*, 2009, **44**, 6447–6450.
8 K. Akhbari, M. Hemmati and A. Morsali, *J. Inorg. Organomet. Polym.*, 2011, **21**, 352–359.
9 X. P. Sun, S. J. Dong and E. K. Wang, *J. Am. Chem. Soc.*, 2005, **127**, 13102–13103.
10 M. Du, C.-P. Li, C.-S. Liu and S.-M. Fang, *Coord. Chem. Rev.*, 2013, **257**, 1282–1305.
11 M. Lin Hu, A. Morsali and L. Aboutorabi, *Coord. Chem. Rev.*, 2011, **225**, 2821–2859.
12 K. Akhbari and A. Morsali, *Inorg. Chem. Acta*, 2009, **363**, 1692–1700.
13 S. L. James, *Chem. Soc. Rev.*, 2003, **32**, 276–288.
14 S. R. Batten, N. R. Champness, X.-M. Chen, J. Garcia-Martinez, S. Kitagawa, L. Öhrström, M. O'Keeffe, M. P. Suh and J. Reedijk, *Pure Appl. Chem.*, 2013, **85**, 1715–1724.
15 B. Moulton and M. J. Zaworotko, *Chem. Rev.*, 2001, **101**, 1629–1658.
16 M. Y. Masoomi and A. Morsali, *Coord. Chem. Rev.*, 2012, **256**, 2921–2943.
17 S. R. Batten, N. R. Champness, X.-M. Chen, J. Garcia-Martinez, S. Kitagawa, L. Öhrström, M. O'Keeffe, M. P. Suh and J. Reedijk, *CrystEngComm*, 2012, **14**, 3001–3004.
18 C. De Wu, A. Hu, L. Zhang and W. Lin, *J. Am. Chem. Soc.*, 2005, **127**, 8940–8941.
19 S. Noro, R. Kitaura, M. Kondo, S. Kitagawa, T. Ishii, H. Matsuzaka and M. Yamashita, *J. Am. Chem. Soc.*, 2002, **124**, 2568–2583.
20 A. M. Shultz, A. A. Sarjeant, O. K. Farha, J. T. Hupp and S. T. Nguyen, *J. Am. Chem. Soc.*, 2011, **133**, 13252–13255.
21 L. J. Murray, M. Dinco and J. R. Long, *Chem. Soc. Rev.*, 2009, **38**, 1294–1314.
22 J. L. Rowsell and O. M. Yaghi, *Angew. Chem.*, 2005, **44**, 4670–4679.
23 S. S. Kaye and J. R. Long, *J. Am. Chem. Soc.*, 2005, **127**, 6506–6507.
24 L. Ma, C. Abney and W. Lin, *Chem. Soc. Rev.*, 2009, **38**, 1248–1256.
25 J. Lee, O. K. Farha, J. Roberts, k. a. Scheidt, S. T. Nguyen and J. T. Hupp, *Chem. Soc. Rev.*, 2009, **38**, 1450–1459.
26 R. Zou, H. Sakurai and Q. Xu, *Angew. Chem.*, 2006, **45**, 2542–2546.
27 S. Hasegawa, S. Horike, R. Matsuda, S. Furukawa, K. Mochizuki, Y. Kinoshita and S. Kitgawa, *J. Am. Chem. Soc.*, 2007, **129**, 2607–2614.
28 J. R. Li, R. J. Kuppler and H. C. Zhou, *Chem. Soc. Rev.*, 2009, **38**, 1477–1504.
29 J. R. Li, J. Sculley and H. C. Zhou, *Chem. Rev.*, 2011, **112**, 869–932.
30 R. C. Huxford, J. D. Rocca and W. Lin, *Curr. Opin. Chem. Biol.*, 2010, **14**, 262–268.
31 J. An, S. J. Geib and N. L. Rosi, *J. Am. Chem. Soc.*, 2009, **131**, 8376–8377.
32 F. Shahangi and K. Akhbari, *Inorg. Chem. Acta*, 2015, **436**, 1–6.
33 F. Shahangi and K. Akhbari, *RSC Adv.*, 2015, **5**, 50778–50782.
34 M. Moeinian and K. Akhbari, *J. Solid State Chem.*, 2015, **225**, 459–463.
35 K. S. Min and M. P. Suh, *J. Am. Chem. Soc.*, 2000, **122**, 6834–6840.
36 K. L. Mulfort and J. T. Hupp, *J. Am. Chem. Soc.*, 2007, **129**, 9604–9605.
37 T. K. Maji, R. Matsuda and S. Kitagawa, *Nat. Mater.*, 2007, **6**, 142–148.
38 Z. Z. Lin, F. L. Jiang, D. Q. Yuan, L. Chen, Y. F. Zhou and M. C. Hong, *Eur. J. Inorg. Chem.*, 2005, 1927–1931.
39 M. Lalonde, W. Bury, O. Karagiaridi, Z. Brown, j. t. Hupp and O. K. Farha, *J. Mater. Chem. A*, 2013, **1**, 5453–5454.
40 C. K. Brozek and M. Dinca, *Chem. Soc. Rev.*, 2014, **43**, 5457–5467.
41 H. Fei, J. F. Cahill, K. A. Prather and S. M. Cohen, *Inorg. Chem.*, 2013, **52**, 4011–4016.
42 M. Kim, J. F. Cahill, H. Fei, K. A. Prather and S. M. Cohen, *J. Am. Chem. Soc.*, 2012, **134**, 18082–18088.
43 S. Das, H. Kim and K. Kim, *J. Am. Chem. Soc.*, 2009, **131**, 3814–3815.
44 A. Nalaparaju and J. Jiang, *J. Phys. Chem.*, 2012, **116**, 6925–6931.
45 J. Fan, L. Gan, H. Kawaguchi, W. Y. Sun and W. X. Tang, *Chem.–Eur. J.*, 2003, **9**, 3965–3973.
46 N. Gimenon and R. Vilar, *Coord. Chem. Rev.*, 2006, **250**, 3161–3189.
47 D. X. Wang, H. Y. He, X. H. Chen, S. Y. Feng, Y. Z. Niu and D. F. Sun, *CrystEngComm*, 2010, **12**, 1041–1043.
48 O. M. Yaghi and H. Li, *J. Am. Chem. Soc.*, 1996, **118**, 295–296.
49 H. J. Choi and M. P. Suh, *J. Am. Chem. Soc.*, 2004, **126**, 15845–15851.
50 Q. Fang, G. Zhu, M. Xue, J. Sun, Y. Wei, S. Qiu and R. Xu, *Angew. Chem., Int. Ed.*, 2005, **44**, 3845–3848.
51 X. Z. Kiang, Y. H. Lee, S. Lobkovsky and E. B. Emmott, *J. Am. Chem. Soc.*, 2000, **122**, 8376–8391.
52 S. R. Halper, L. Do, J. R. Stork and S. M. Cohen, *J. Am. Chem. Soc.*, 2006, **128**, 15255–15267.

53 S. Y. Wan, Y. T. Huang, Y. Z. Li and W. Y. Sun, *Microporous Mesoporous Mater.*, 2004, **73**, 101–108.
54 M. Shu, C. Tu, W. Xu, H. Jin and J. Sun, *Cryst. Growth Des.*, 2006, **6**, 1890–1896.
55 J. Chen, C. P. Li, J. Shang and M. Du, *Inorg. Chem. Commun.*, 2012, **15**, 172–175.
56 M. Sadakiyo, H. Kasai, K. Kato, M. Takata and M. Yamaudi, *J. Am. Chem. Soc.*, 2014, **136**, 1702–1705.
57 L. Carlucci, G. Ciani, S. Maggini, D. H. Proserpio and M. Visconti, *Chem.–Eur. J.*, 2010, **16**, 12328–12341.
58 M. L. Feng, D. N. Kong, Z. L. Xie and X. Y. Huang, *Angew. Chem.*, 2008, **74**, 8623–8626.
59 P. Wang, J. P. Ma, Y. B. Dong and R. Q. Huang, *J. Am. Chem. Soc.*, 2007, **129**, 10620–10621.
60 R. Mark and W. N. Findley, *Polym. Eng. Sci.*, 1978, **18**, 6–15.
61 J. An and N. L. Rosi, *J. Am. Chem. Soc.*, 2010, **132**, 5578–5579.
62 L. Carlucci, G. Ciani, S. Maggini, D. M. Proserpio and M. Visconti, *Chem.–Eur. J.*, 2010, **16**, 12328–12341.
63 T. F. Liu, J. Lu, C. Tian, M. Cao, Z. Lin and R. Cao, *Inorg. Chem.*, 2011, **50**, 2264–2271.
64 J. Yu, Y. Cui, C. Wu, Y. Yang, Z. Wang, M. O'Keeffe, B. Chen and G. Qian, *Angew. Chem.*, 2012, **51**, 1–5.
65 S. Xiong, S. Li, S. Wang and Z. Wang, *CrystEngComm*, 2011, **13**, 7236–7245.
66 R. X. Yao, X. Xu and X. M. Zhang, *Chem. Mater.*, 2012, **24**, 303–310.
67 H. Zhang, Y. Lu, Z. Zhang, H. Fu, Y. Li, D. Volkmer, D. Denysenko and E. Wang, *Chem. Commun.*, 2012, **48**, 7295–7297.
68 D. Banerjee, S. J. Kim, H. Wu, W. Xu, L. A. Borkowski, J. Li and J. B. Parise, *J. Am. Chem. Soc.*, 2011, **50**, 208–212.
69 D. W. Breck and R. E. Krieger, *Struct. Chem.*, 1984, **ix**, 771.
70 Y. Liu, V. C. Kravtsov, R. Larsen and M. Eddaoudi, *Chem. Commun.*, 2006, 1488–1590.
71 M. Eddaoudi, J. F. Eubank, Y. Liu, V. C. Kravtsov, R. W. Larsen and J. A. Brant, *Stud. Surf. Sci. Catal.*, 2007, **170B**, 2021–2029.
72 X. Zhao, X. Bu, T. Wu, S. T. Zheng, L. Wang and P. Feng, *Nat. Commun.*, 2013, **3344**, 1–9.
73 J. P. Ma, Y. Yu and Y. B. Dong, *Chem. Commun.*, 2012, **48**, 2946–2948.
74 R. Custelcean, T. J. Havelock and B. A. Moyer, *Inorg. Chem.*, 2006, **45**, 6446–6452.
75 S. R. Oliver, *Chem. Soc. Rev.*, 2009, **38**, 1868–1881.
76 US Department of Health and Human Services, *Toxicological Profile for Chromium, Public Health Service Agency for Toxic Substances and Disease Registry*, Washington, DC, 1991.
77 E. A. Katayev, Y. A. Ustynyuk and J. L. Sessler, *Coord. Chem. Rev.*, 2006, **250**, 3004–3037.
78 P. F. Shi, B. Zhao, G. Xiong, Y. L. Hou and P. Cheng, *Chem. Commun.*, 2012, **48**, 8231–8233.
79 E. T. Urbansky, *Environ. Sci. Pollut. Res. Int.*, 2002, **9**, 187–192.
80 H. Fei, M. R. Bresler and S. R. Oliver, *J. Am. Chem. Soc.*, 2011, **133**, 11110–11113.
81 H. R. Fu, Z. X. Xu and J. Zhang, *Chem. Mater.*, 2015, **27**, 205–210.
82 X. Li, H. Xu, F. Kong and R. Wang, *Angew. Chem., Int. Ed.*, 2013, **52**, 13769–13773.
83 V. Guillerm, F. Ragon, M. Dan-Hardi, T. Devic, M. Vishnuvarthan, B. Campo, A. Vimont, G. Clet, Q. Yang, G. Maurin, G. Férey, A. Vittadini, S. Gross and C. Serre, *Angew. Chem., Int. Ed.*, 2012, **51**, 9267–9271.
84 H. Furukawa, F. Gandara, Y. B. Zhang, J. Jiang, W. L. Queen, M. R. Hudson and O. M. Yaghi, *J. Am. Chem. Soc.*, 2014, **136**, 4369–4381.
85 K. M. Choi, H. M. Jeong, J. H. Park, Y.-B. Zhang, J. K. Kang and O. M. Yaghi, *ACS Nano*, 2014, **8**, 7451–7457.
86 Q. Zhang, J. Yu, J. Cai, L. Zhang, Y. Cui, Y. Yang, B. Chen and G. Qian, *Chem. Commun.*, 2015, **51**, 14732–14734.
87 A. V. Desai, B. Manna, A. Karmakar, A. Sahu and S. K. Ghosh, *Angew. Chem., Int. Ed.*, 2016, **55**, 7811–7815.
88 F. X. L. Xamena, O. Casanova, R. G. Tailleur, H. Garcia and A. Corma, *J. Catal.*, 2008, **225**, 220–227.
89 S. Wang, L. Li, J. Zhang, X. Yuan and C. Y. Su, *Mater. Chem.*, 2011, **21**, 7098–7104.
90 B. K. Banik, M. Chapa, J. Marquez and M. Cardona, *Tetrahedron Lett.*, 2005, **46**, 2341–2343.
91 H. Fei, D. L. Rogow and S. R. J. Oliver, *J. Am. Chem. Soc.*, 2010, **132**, 7202–7209.
92 Q. Y. Yang, K. Li, J. Luo, M. Pan and C. Y. Su, *Chem. Commun.*, 2011, **47**, 4234–4236.
93 B. Manna, A. K. Chaudhari, B. Joorder, A. Karmaker and S. K. Ghosh, *Angew. Chem.*, 2013, **52**, 998–1002.
94 X. P. Li, J. Y. Zhang, M. Pan, S. R. Zheng, Y. Liu and C. Y. Su, *Inorg. Chem.*, 2007, **46**, 4617–4625.
95 J. J. Baldovi, E. Coronado, A. G. Arino, C. Gamer, M. G. Marques and G. M. Espallargas, *Chem.–Eur. J.*, 2014, **20**, 10695–10702.
96 Q. K. Liu, J. P. Ma and Y. B. Dong, *Chem. Commun.*, 2011, **47**, 7185–7187.
97 E. Q. Procopio, F. Linares, C. Montoro, V. Colombo, A. Maspero, E. Barea and J. A. R. Navarro, *Angew. Chem.*, 2010, **122**, 7456–7469.
98 Y. X. Tan, Y. P. He and J. Zhang, *Chem. Commun.*, 2011, **47**, 10647–10649.
99 Y. X. Tan, Y. P. He and J. Zhang, *Chem. Commun.*, 2014, **50**, 6153–6156.
100 D. T. Genna, A. G. Wong-Fey, A. J. Matzger and M. S. Sanford, *J. Am. Chem. Soc.*, 2013, **135**, 10586–10589.
101 S. Beheshti and A. Morsali, *RSC Adv.*, 2014, **4**, 41825–41830.
102 S. Beheshti and A. Morsali, *RSC Adv.*, 2014, **4**, 37036–37040.
103 F. Nouar, J. Eckert, J. F. Eubank, P. Forster and M. Eddaoudi, *J. Am. Chem. Soc.*, 2009, **131**, 2864–2870.
104 G. Calleja, J. A. Botas, M. S. Sanchez and M. G. Orcajo, *Int. J. Hydrogen Energy*, 2010, **35**, 9916–9923.
105 S. Yang, G. S. B. Martin, J. J. Titman, A. J. Blake, D. R. Allan, N. R. Champness and M. Schroder, *Inorg. Chem.*, 2011, **50**, 9374–9384.
106 S. Yang, X. Lin, A. J. Blake, G. S. Walker, P. Hubberstay, N. R. Champness and M. Schroder, *Nat. Chem.*, 2009, **1**, 487–493.
107 K. L. Mulfort, O. K. Farha, C. L. Stern, A. A. Sarjeant and J. T. Hupp, *J. Am. Chem. Soc.*, 2009, **131**, 3866–3868.

108 Y. Liu, V. C. Kravtsov and M. Eddaoudi, *Angew. Chem.*, 2008, **47**, 8446–8449.
109 S. Yang, S. K. Callear, A. J. Ramirez-Cuesta, W. I. F. David, J. Sun, A. J. Blake, N. R. Champness and M. Schroder, *Faraday Discuss.*, 2011, **151**, 19–36.
110 J. An and N. L. Rosi, *J. Am. Chem. Soc.*, 2010, **132**, 5578–5579.
111 C. Chen, J. Kim, D. A. Yang and W. S. Ahn, *Chem. Eng. J.*, 2011, **168**, 1134–1139.
112 D. F. Sava, V. C. Kravtsov, F. Nouar, L. Wojtas, J. F. Eubank and M. Eddaoudi, *J. Am. Chem. Soc.*, 2008, **130**, 3768–3770.
113 X. R. Hao, X. L. Wang, Z. M. Su, K. Z. Shao, Y. H. Zhao, Y. Q. Lan and Y. M. Fu, *Dalton Trans.*, 2009, **40**, 8562–8566.
114 Z. J. Li, S. K. Khani, K. Akhbari, A. Morsali and P. Retailleau, *Microporous Mesoporous Mater.*, 2014, **199**, 93–98.
115 T. Z. Zhang, Z. M. Zhang, Y. Lu, H. Fu and E. B. Wang, *CrystEngComm*, 2013, **15**, 459–462.
116 K. Akhbari and A. Morsali, *Dalton Trans.*, 2013, **42**, 4786–4789.
117 F. J. Ma, S. X. Liu, D. D. Liang, G. J. Ren, F. Wei, Y. G. Chen and Z. M. Su, *Solid State Chem.*, 2011, **184**, 3034–3039.
118 J. S. Qin, S. R. Zhang, D. Y. Du, P. Shen, S. J. Bao, Y. Q. Lan and Z. M. Su, *Chem.–Eur. J.*, 2014, **20**, 5625–5630.
119 W. G. Lu, L. Jiang, X. L. Feng and T. B. Lu, *Inorg. Chem.*, 2009, **48**, 6997–6999.
120 S. Liu, J. Li and F. Luo, *Inorg. Chem. Commun.*, 2010, **13**, 870–872.
121 J. Cao, Y. Gao, Y. Wang, C. Du and Z. Liu, *Chem. Commun.*, 2013, **49**, 6897–6899.
122 S. Dang, E. Ma, Z. M. Sun and H. Zhang, *Mater. Chem.*, 2011, **22**, 16920–16926.
123 Z. Chen, Y. Sun, L. Zhang, D. Sun, F. Liu, Q. Meng, R. Wang and D. Sun, *Chem. Commun.*, 2013, **49**, 11557–11559.
124 Y. Liu, G. Li, X. Li and Y. Cui, *Angew. Chem.*, 2007, **119**, 6417–6420.
125 J. Yu, Y. Cui, H. Xu, Y. Yang, Z. Wang, B. Chen and G. Qian, *Nat. Commun.*, 2013, **3719**, 1–7.